Title

Products of the OH Radical-Initiated Reactions of Furan, 2- and 3-Methylfuran, and 2,3- and 2,5-Dimethylfuran in the Presence of NO

Journal

The Journal of Physical Chemistry A, 118(2)

ISSN

1089-5639

Authors

Aschmann, Sara M
Nishino, Noriko
Arey, Janet
et al.

Publication Date

2014-01-16

DOI

10.1021/jp410345k

Peer reviewed

THE JOURNAL OF PHYSICAL CHEMISTRY A

Article

pubs.acs.org/JPCA

Products of the OH Radical-Initiated Reactions of Furan, 2- and 3-Methylfuran, and 2,3- and 2,5-Dimethylfuran in the Presence of NO

Sara M. Aschmann, Noriko Nishino,[†] Janet Arey,*[,‡] and Roger Atkinson*[,‡]

Air Pollution Research Center, University of California, Riverside, California 92521, United States

Supporting Information

ABSTRACT: Products of the gas-phase reactions of OH radicals with furan, furan-d_4, 2- and 3-methylfuran, and 2,3- and 2,5-dimethylfuran have been investigated in the presence of NO using direct air sampling atmospheric pressure ionization tandem mass spectrometry (API-MS and API-MS/MS), and gas chromatography with flame ionization and mass spectrometric detectors (GC−FID and GC−MS) to analyze samples collected onto annular denuders coated with XAD solid adsorbent and further coated with *O*-(2,3,4,5,6-pentafluorobenzyl)-hydroxylamine for derivatization of carbonyl-containing compounds to their oximes. The products observed were unsaturated 1,4-dicarbonyls, unsaturated carbonyl-acids and/or hydroxy-furanones, and from 2,5-dimethylfuran, an unsaturated carbonyl-ester. Quantification of the unsaturated 1,4-dicarbonyls was carried out by GC−FID using 2,5-hexanedione as an internal standard, and the measured molar formation yields were: HC(O)CH=CHCHO (dominantly the *E*-isomer) from OH + furan, 75 ± 5%; $CH_3C(O)CH=CHCHO$ (dominantly the *E*-isomer) from OH + 2-methylfuran, 31 ± 5%; $HC(O)C(CH_3)=CHCHO$ (a *E*-/*Z*-mixture) from OH + 3-methylfuran, 38 ± 2%; and $CH_3C(O)C(CH_3)=CHCHO$ from OH + 2,3-dimethylfuran, 8 ± 2%. In addition, a formation yield of 3-hexene-2,5-dione from OH + 2,5-dimethylfuran of 27% was obtained from a single experiment, in good agreement with a previous value of 24 ± 3% from GC−FID analyses of samples collected onto Tenax solid adsorbent without derivatization.

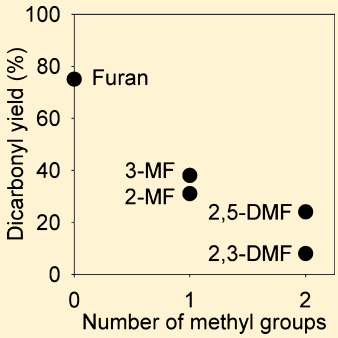

INTRODUCTION

Furan and alkylfurans are emitted directly into the atmosphere as well as being formed in situ from atmospheric degradation of certain other volatile organic compounds.[1−3] Furan and alkylfurans are transformed further in the atmosphere by reactions with OH radicals, NO_3 radicals, O_3 and Cl atoms,[4] and the products of their OH radical-initiated reactions include unsaturated 1,4-dicarbonyls.[5−8] These reactions may therefore be useful as potentially clean in situ laboratory sources of unsaturated 1,4-dicarbonyls, which are otherwise not readily available.[6,7] In this work, we have extended our previous measurements of the rate constants for the reactions of OH radicals with 2- and 3-methylfuran and 2,3- and 2,5-dimethylfuran and of the formation yield of 3-hexene-2,5-dione from OH + 2,5-dimethylfuran[7] to investigate the products formed from OH + furan, 2- and 3-methylfuran and 2,3-dimethylfuran in the presence of NO. Additional product analyses are presented for OH + 2,5-dimethylfuran for comparison with the furan, 2- and 3-methylfuran and 2,3-dimethylfuran reactions. The loss processes of the unsaturated 1,4-dicarbonyls, which are also products of OH + aromatic hydrocarbon reactions,[9−14] were also explored.

EXPERIMENTAL METHODS

Experiments were carried out at 296 ± 2 K and ∼735 Torr pressure of dry purified air in ∼7000 L Teflon chambers, each equipped with two parallel banks of black lamps for irradiation at >300 nm and with a Teflon-coated fan to ensure rapid mixing during the introduction of chemicals into the chamber. OH radicals were generated by the photolysis of methyl nitrite (CH_3ONO), and NO was also included in the reactant mixtures to suppress the formation of O_3 and hence of NO_3 radicals. Unless noted otherwise, all irradiations were carried out at a light intensity corresponding to an NO_2 photolysis rate of 0.14 min^{-1}.

Analyses by Gas Chromatography. A series of CH_3ONO−NO−furan−air irradiations were carried out, with initial concentrations (molecules cm^{-3}) of CH_3ONO and NO, ∼1.2 × 10^{14} each; furan, (1.91−2.54) × 10^{13}; and 2,5-hexanedione (used as an internal standard; see below), (6.10−8.50) × 10^{12}. Each experiment involved a single irradiation of duration 1.5−8 min, resulting in 35−64% consumption of the initially present furan. Three preliminary experiments with 2,3-dimethylfuran were carried out with similar initial CH_3ONO, NO and 2,3-dimethylfuran concentrations, with the 2,5-hexanedione internal standard being present initially in one experiment (2.27 × 10^{12} molecules cm^{-3}) and being added after the irradiation in the other two (2.30 × 10^{12} and 8.99 × 10^{12} molecules cm^{-3}). In these three experiments, the mixtures were irradiated for 3−4 min, with 49−61% consumption of 2,3-dimethylfuran.

The concentrations of the furans and 2,5-hexanedione (and 3-hexene-2,5-dione in the OH + 2,5-dimethylfuran reaction) were measured before and after the irradiation by gas

Received: October 18, 2013
Revised: December 12, 2013
Published: December 31, 2013

Scheme 1

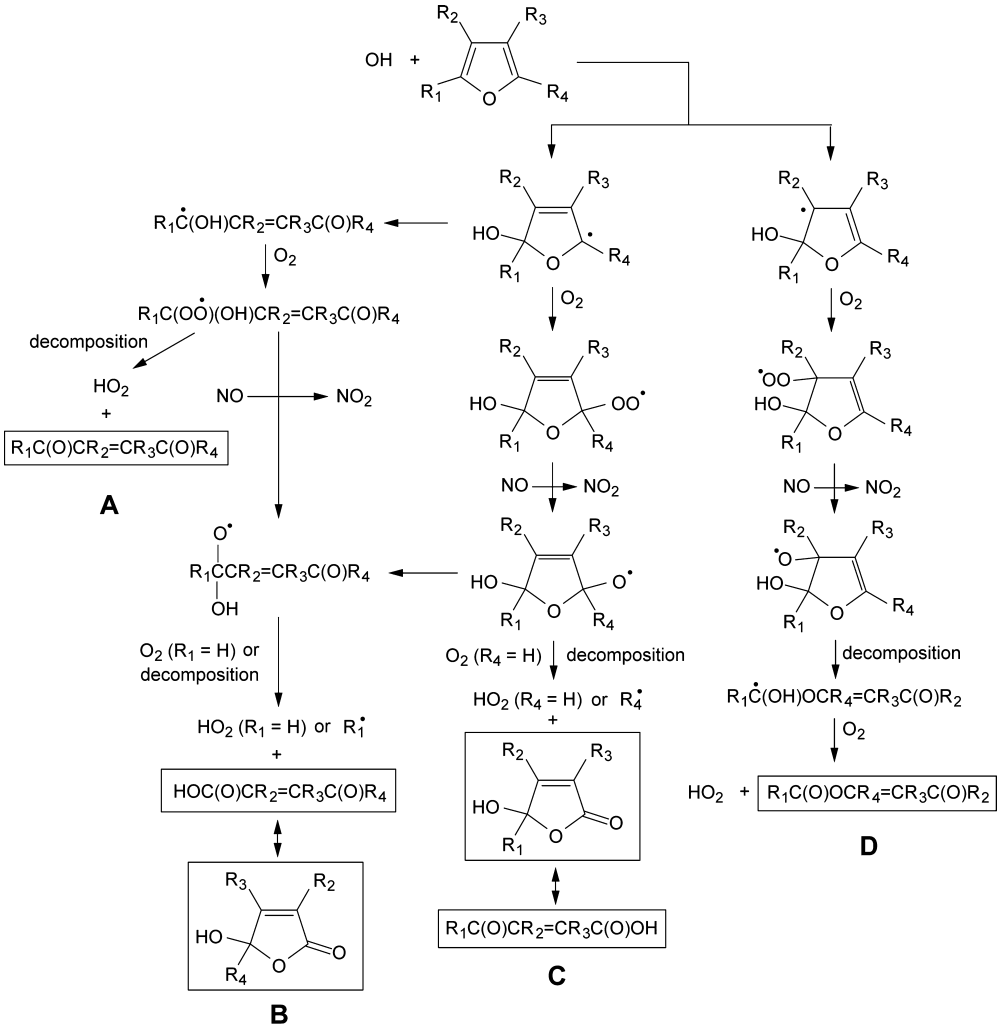

chromatography with flame ionization detection (GC−FID). Gas samples of 100 cm^3 volume were collected from the chamber onto Tenax-TA solid adsorbent, with subsequent thermal desorption at ∼205 °C onto a 30 m DB-1701 megabore column, temperature programmed from −40 °C at 8 °C min^{-1}. For the analysis of furan, gas samples were collected from the chamber into a 100 cm^3 volume all-glass gastight syringe and transferred via a 1 cm^3 gas sampling loop onto a 30 m DB-5 megabore column initially held at −25 °C and then temperature programmed at 8 °C min^{-1}. Replicate analyses before and after the irradiations typically agreed to within 3%.

Samples were collected, starting immediately after the lights were turned off, for 60 min at 15 L min^{-1} using an XAD-coated denuder, further coated with *O*-(2,3,4,5,6-pentafluorobenzyl)-hydroxylamine (PFBHA) prior to sampling,[13,15] and extracted as described previously.[13] The extracts were analyzed by positive chemical ionization gas chromatography−mass spectrometry (PCI GC−MS) and GC−FID, both analyses using 30 m DB-5 columns. The PCI GC−MS analyses used an Agilent 6890N GC interfaced to an Agilent 5975 Inert XL Mass Selective Detector operated with methane as the reagent gas. Each carbonyl group derivatized to an oxime added 195 mass units to the compound's molecular weight (mw), and methane-PCI gave characteristic protonated molecules ($[M+H]^+$) and smaller adduct ions at $[M+29]^+$ and $[M+41]^+$.[13]

An analogous CH_3ONO−NO−3-methyl-2-butenal−air irradiation was carried out, with 2,5-hexanedione present as an internal standard, to measure the glyoxal formation yield from OH + 3-methyl-2-butenal and compare it with the yield previously measured using in situ Fourier transform infrared (FTIR) spectroscopy.[16] The initial concentrations (molecules cm^{-3}) were CH_3ONO and NO, ∼1.2×10^{14} each; 3-methyl-2-butenal, 2.11×10^{13}; and 2,5-hexanedione, 4.06×10^{12}. The mixture was irradiated for 3 min, resulting in 50% reaction of the initially present 3-methyl-2-butenal. The concentrations of 3-methyl-2-butenal and 2,5-hexanedione were measured by GC−FID analyses of samples collected onto Tenax solid adsorbent, and those of the dioximes of 2,5-hexanedione and glyoxal were measured by GC−FID analyses of an extract of a PFBHA-coated denuder sample, as described above.

Analyses by API-MS/MS. CH_3ONO−NO−furan−air irradiations were carried out during which the chamber contents were sampled through a 25 mm diameter × 75 cm length Pyrex tube at ∼20 L min^{-1} directly into the API-MS source. The operation of the API-MS in the MS (scanning) and MS/MS [with collision activated dissociation (CAD)] modes has been described previously.[7,17] Both positive and negative ion modes were used in this work. In positive ion mode, protonated water hydrates ($H_3O^+(H_2O)_n$) generated by the corona discharge in the chamber diluent air were responsible

dx.doi.org/10.1021/jp410345k | J. Phys. Chem. A 2014, 118, 457−466

Table 1. Products Formed from the Furans Studied from API-MS and API-MS/MS Analyses

	molecular weight of potential products (Scheme 1)				
furan	pathway A	pathway B	pathway C	pathway D	observed products from API-MS analyses and ion peak attribution
furan	84	100	100	100	84,[a,b] HC(O)CH=CHCHO 100,[a,c] HC(O)CH=CHC(O)OH and/or isomer[d]
furan-d_4	88	103	103	104	88,[a] DC(O)CD=CDCDO 103,[a,c] DC(O)CD=CDC(O)OH and/or isomer[d]
2-methylfuran	98	100, 114	100, 114	114	98,[a,b] $CH_3C(O)CH$=CHCHO 100,[a,c] HC(O)CH=CHC(O)OH and/or isomer[d] 114,[a,c] $CH_3C(O)CH$=CHC(O)OH and/or isomer[d]
3-methylfuran	98	114	114	114	98,[a,e] HC(O)$C(CH_3)$=CHCHO 114[a,c] HC(O)$C(CH_3)$=CHC(O)OH and/or isomer[d]
2,3-dimethylfuran	112	114, 128	114, 128	128	112,[a,e] $CH_3C(O)C(CH_3)$=CHCHO 114,[a,c] HC(O)C=$C(CH_3)$C(O)OH and/or isomer[d] 128,[a,c] $CH_3C(O)C(CH_3)$=CHC(O)OH and/or isomer[d]
2,5-dimethylfuran	112	114	114	128	112[a,e] $CH_3C(O)CH$=CHC(O)CH_3 114,[a,c] $CH_3C(O)CH$=CHC(O)OH and/or isomer[d] 128,[a] $CH_3C(O)OCH$=CHC(O)CH_3

[a]Observed in positive ion mode. [b]Small NO_2^- adduct peak observed in negative ion mode (see Figure 2 and its caption for the case of 2-methylfuran). [c]Observed in negative ion mode. [d]See Scheme 1, pathways B and C. [e]Small ion peak present in negative ion mode which could have been the NO_2^- adduct ion.

for the formation of protonated molecules ($[M+H]^+$), water adduct ions $[M+H+H_2O]^+$, and protonated homo- and heterodimers,[7,17] while in negative ion mode O_2^-, NO_2^- and NO_3^- ions were responsible for formation of adduct ions.[17] The initial concentrations and experimental conditions were similar to those of the product studies, except that 2,5-hexanedione was not present.

Chemicals. The chemicals used, and their stated purities, were 2,3-dimethylfuran (99%), 2,5-dimethylfuran (99%), furan (99+%), 2,5-hexanedione (98+%), 3-methyl-2-butenal (97%), 2-methylfuran (99%), *O*-(2,3,4,5,6-pentafluorobenzyl)-hydroxylamine hydrochloride (>98%), 1,2,3-trimethylbenzene (90%), *o*-xylene (97%), and *p*-xylene (99+%), Aldrich; *E*-3-hexene-2,5-dione (GC−MS analyses of its dioximes in samples collected from the chamber onto a PFBHA-coated denuder showed no detectable *Z*-isomer), Hestia Laboratories Inc.; furan-d_4, (98 atom % D), Isotec; 3-methylfuran (98%), Arcos Organic; 5-hydroxy-2-pentanone (≥96%), TCI America; and NO (≥99.0%), Matheson Gas Products. Methyl nitrite was prepared as described by Taylor et al.[18] and stored at 77 K under vacuum.

RESULTS AND DISCUSSION

Our recent product study of the OH + 2,5-dimethylfuran reaction[7] showed the formation of the unsaturated 1,4-dicarbonyl 3-hexene-2,5-dione (mw 112) plus additional products of mw 114 and mw 128 in both the presence and absence of NO_x, with the 3-hexene-2,5-dione yield being higher in the absence of NO_x (34 ± 3%) than in the presence of NO_x (24 ± 3%, independent of initial NO concentration over the range (2.4−24) × 10^{13} molecules cm^{-3}).[7] The formation of 1,4-butenedial from OH + furan,[5,6] 4-oxo-2-pentenal from OH + 2-methylfuran,[5,6] 2-methyl-1,4-butenedial from OH + 3-methylfuran,[6] and 3-hexene-2,5-dione from OH + 2,5-dimethylfuran[7] implies that these unsaturated 1,4-dicarbonyls are formed after initial OH addition at the 2- or 5-positions (pathway A in Scheme 1).[5−7] However, the formation of additional products from OH + 2,5-dimethylfuran and the effect of NO_x on the 3-hexene-2,5-dione yield showed that additional reaction pathways are operative,[7] and these are denoted as pathways B, C and D in Scheme 1. Table 1 lists the molecular weights of the potential products formed from these four pathways, noting that for OH radical addition at the 2- or 5-positions, different molecular weight products are formed from 2-methylfuran and 2,3-dimethylfuran through pathways B and C depending on whether the initial OH radical addition is at the 2- or 5-position. OH radical addition at the 3- or 4-positions would lead to the same carbonyl-ester products as formed after addition at the 2- or 5-positions, respectively, via pathway D (see Supporting Information to ref 7).

Analysis by API-MS. In positive ion mode prior to reaction, ion peaks due to the furans were observed at M^+, $[M+H]^+$ and $[M+NO]^+$. Additional ion peaks were observed after reaction, and API-MS spectra from the reactions of furan, 2- and 3-methylfuran and 2,3-dimethylfuran during the initial stages of the reactions are shown in Figure 1. An analogous API-MS spectrum from the 2,5-dimethylfuran reaction was presented in Aschmann et al.[7] The assignments of these ion peaks, based on API-MS/MS spectra, are noted in the caption to Figure 1 and the molecular weights of the products observed, and whether they were observed in negative ion mode as well as in positive ion mode, are listed in Table 1. An example of the negative ion mode API-MS spectra obtained is shown in Figure 2 for the OH + 2-methylfuran reaction, and the ion peak assignments are given in the caption to Figure 2. The API-MS negative ion mode spectra for furan, furan-d_4, 3-methylfuran, and 2,3- and 2,5-dimethylfuran were analogous, with the ion peaks being assigned to either one (furan, furan-d_4, 3-methylfuran, and 2,5-dimethylfuran) or two (2-methylfuran and 2,3-dimethylfuran) product masses (Table 1).

All of the furans studied here show the presence of product masses consistent with those expected from pathway A and pathways B and/or C in Scheme 1, noting that pathways B and C lead to the same product masses. Pathway D can only be discriminated from pathways B and C for the furan-d_4 and 2,5-dimethylfuran reactions (Table 1). The API-MS spectra showed evidence for the occurrence of pathway D in the OH + 2,5-dimethylfuran reaction (ref 7 and Table 1), but not in the OH + furan-d_4 reaction. The products attributed to formation via pathways B and/or C were observed in both positive and

dx.doi.org/10.1021/jp410345k | J. Phys. Chem. A 2014, 118, 457−466

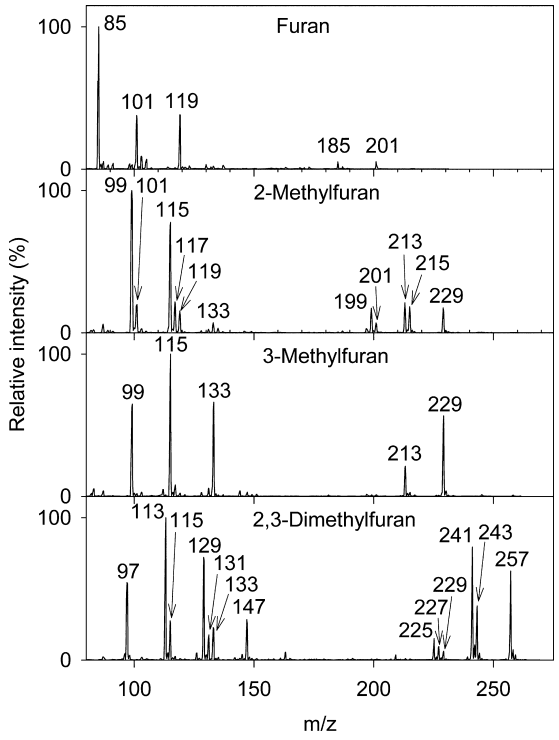

Figure 1. Positive mode API-MS spectra of irradiated $CH_3ONO-NO-$furan$-$air mixtures. The ion peaks are attributed to: OH + furan, m/z 85, $[84+H]^+$; m/z 101, $[100+H]^+$; m/z 119, $[100+H+H_2O]^+$; m/z 185, $[84+100+H]^+$; and m/z 201, $[100+100+H]^+$; OH + 2-methylfuran, m/z 99, $[98+H]^+$; m/z 101, $[100+H]^+$; m/z 115, $[114+H]^+$; m/z 117, $[98+H+H_2O]^+$; m/z 119, $[100+H+H_2O]^+$; m/z 133, $[114+H+H_2O]^+$; m/z 199, $[98+100+H]^+$; m/z 201, $[100+100+H]^+$; m/z 213, $[98+114+H]^+$; m/z 215, $[100+114+H]^+$; and m/z 229, $[114+114+H]^+$; OH + 3-methylfuran, m/z 99, $[98+H]^+$; m/z 115, $[114+H]^+$; m/z 133, $[114+H+H_2O]^+$; m/z 213, $[98+114+H]^+$; and m/z 229, $[114+114+H]^+$; OH + 2,3-dimethylfuran, m/z 97, [2,3-dimethylfuran+H]$^+$; m/z 113, $[112+H]^+$; m/z 115, $[114+H]^+$; m/z 129, $[128+H]^+$; m/z 131, $[112+H+H_2O]^+$; m/z 133, $[114+H+H_2O]^+$; m/z 147, $[128+H+H_2O]^+$; m/z 225, $[112+112+H]^+$; m/z 227, $[112+114+H]^+$; m/z 229, $[114+114+H]^+$; m/z 241, $[112+128+H]^+$; m/z 243, $[114+128+H]^+$; and m/z 257, $[128+128+H]^+$.

negative ion modes, whereas those from pathways A and D were observed mainly in positive ion mode (see footnotes to Table 1).

Analyses by GC−MS. GC−MS analyses of extracts of samples collected using PFBHA-coated denuders showed the presence of the expected unsaturated 1,4-dicarbonyls (pathway A in Scheme 1, and Table 1). A PCI GC−MS total ion chromatogram (TIC) is shown in Figure 3 for the furan reaction, and Figures S1−S4 in the Supporting Information show the PCI GC−MS TICs for 2- and 3-methylfuran and 2,3- and 2,5-dimethylfuran. Most experiments were carried out with the internal standard 2,5-hexanedione present in the initial reactant mixtures (i.e., before reaction). The rate constant for the reaction of OH radicals with 2,5-hexanedione has been measured to be $(7.13 \pm 0.34) \times 10^{-12}$ cm^3 molecule^{-1} s^{-1} at 298 K,[19] and hence 2,5-hexanedione is less reactive toward OH radicals than the furans studied here, by factors of 6−18.[4,7] Based on the measured concentrations of 2,5-hexanedione before and after reaction, the percentages of 2,5-hexanedione, which were consumed by reaction were 11−17% in the furan reactions and ≤6% in the 2- and 3-methylfuran and 2,3- and

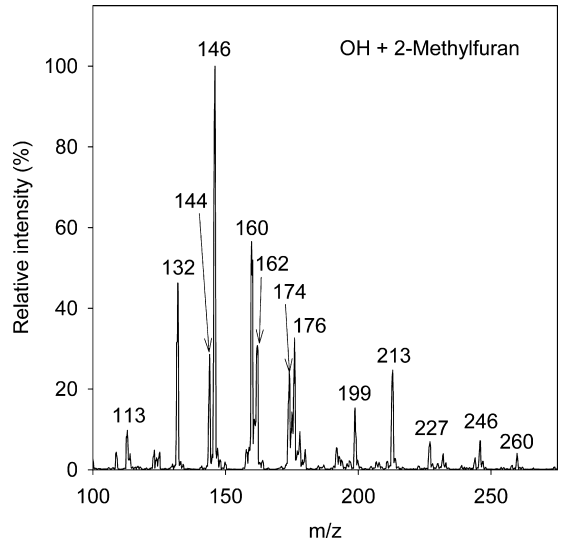

Figure 2. Negative mode API-MS spectrum of an irradiated $CH_3ONO-NO-$2-methylfuran$-$air mixture. The ion peaks are attributed to: m/z 132, $[100+O_2]^-$; m/z 144, $[98+NO_2]^-$; m/z 146, $[100+NO_2]^-$ and $[114+O_2]^-$; m/z 160, $[114+NO_2]^-$; m/z 162, $[100+NO_3]^-$; m/z 174, $[114+60]^-$; m/z 176, $[114+NO_3]^-$; m/z 199, $[100+100-H]^-$; m/z 213, $[100+114-H]^-$; m/z 227, $[114+114-H]^-$; m/z 246, $[100+114+O_2]^-$ and $[100+100+NO_2]^-$; and m/z 260, $[114+114+O_2]^-$ and $[100+114+NO_2]^-$.

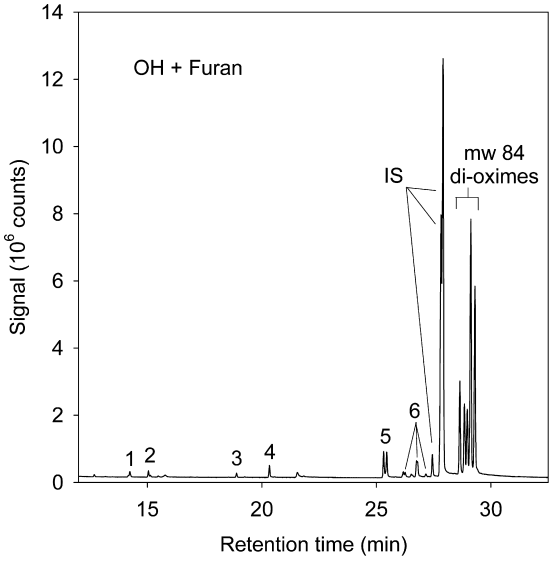

Figure 3. Positive chemical ionization GC−MS total ion chromatogram (TIC) of an extract of a PFBHA-coated denuder sample collected after 4 min irradiation of a $CH_3ONO-NO-$furan$-$2,5-hexanedione (internal standard, IS)$-$air mixture, with 38% consumption of the initially present furan. IS = dioximes of 2,5-hexanedione, the internal standard; peak #1, mono-oxime of molecular weight (mw) 92 carbonyl; peak #2, mono-oxime of $CH_3C(O)CH_2CHO$ (mw 86) formed from OH + 2,5-hexanedione, the internal standard; peaks #3 and #4, from derivatizing agent; peaks #5, dioximes of glyoxal; peaks #6, dioximes of $CH_3C(O)CH_2CHO$ (mw 86) formed from OH + 2,5-hexanedione; and mw 84 dioximes of HC(O)CH═CHCHO.

2,5-dimethylfuran reactions, consistent with expectations based on the relative reactivities of 2,5-hexanedione and the furans and the fractions of the furans reacted. The unsaturated 1,4-dicarbonyls and glyoxal, methylglyoxal, 2,3-butanedione and 3-

dx.doi.org/10.1021/jp410345k | J. Phys. Chem. A 2014, 118, 457−466

oxobutanal [$CH_3C(O)CH_2CHO$] were identified by matching GC retention times and mass spectra of their oximes with those generated in situ from OH radical-initiated reactions of *o*-xylene, *p*-xylene, 1,2,3-trimethylbenzene, and 5-hydroxy-2-pentanone, which form these compounds.[13,20,21] A major expected product of OH + 2,5-hexanedione is 3-oxobutanal, and this mw 86 dicarbonyl was observed in all PCI GC−MS analyses when 2,5-hexanedione was present prior to reaction (and in much lesser amounts when 2,5-hexanedione was not present prior to reaction, presumably due to carry-over from previous experiments).

The products observed from the OH + furan reactions by GC−MS were then as follows: from furan: 1,4-butenedial [HC(O)CH=CHCHO], glyoxal, and a mw 92 carbonyl; from 2-methylfuran, 4-oxo-2-pentenal [$CH_3C(O)CH$=CHCHO], glyoxal, methylglyoxal, a mw 100 product, and a mw 114 product(s); from 3-methylfuran, 2-methyl-1,4-butenedial [HC(O)C(CH_3)=CHCHO], glyoxal, methylglyoxal, and mw 114 product(s); from 2,3-dimethylfuran, 3-methyl-4-oxo-2-pentenal [$CH_3C(O)C(CH_3)$=CHCHO], glyoxal, methylglyoxal, biacetyl, mw 60 carbonyl (most likely a hydroxycarbonyl and hence glycolaldehyde, $HOCH_2CHO$), mw 114 carbonyl, plus other unidentified peaks; and from 2,5-dimethylfuran, 3-hexene-2,5-dione [$CH_3C(O)CH$=$CHC(O)CH_3$], glyoxal, methylglyoxal, and mw 114 carbonyl. Based on the PCI GC−MS TICs, glyoxal, methylglyoxal and 2,3-butanedione formation was minor in all cases, and could have arisen as second-generation products.[5] Bierbach et al.[5] also observed the formation of glyoxal from OH + furan (with a formation yield of 8.2% in the initial stages of reaction, decreasing to 4.4% at higher extents of reaction), and of glyoxal and methylglyoxal from OH + 2-methylfuran (with formation yields of 1.5−4.8% and 1.6−2.3%, respectively, both increasing with the extent of reaction), both reactions being studied in the absence of NO_x.

The dioxime profiles from the GC−MS analyses can be compared to those for the reactions of OH radicals with aromatic hydrocarbons,[7,13,20] where the unsaturated 1,4-dicarbonyls are assumed to be formed in the *Z*-configuration based on the observation that 3-hexene-2,5-dione is formed from OH + *p*-xylene and 1,2,4-trimethylbenzene in the *Z*-configuration,[7,11] recognizing that *Z*-/*E*-photoisomerization occurs and that short irradiation times are hence necessary to maintain the initial *Z*-/*E*-distribution. For dicarbonyls not containing a C=C bond, there are up to four dioximes, depending on symmetry, these being *syn,syn*; *syn,anti*; *anti,syn* and *anti,anti*. For the unsaturated 1,4-dicarbonyls that exist as *Z*- and *E*-isomers, there are up to eight dioximes, with six for those with a center of symmetry such as 1,4-butenedial and 3-hexene-2,5-dione, noting that because of coelution and/or dominance of certain configurations, not all possible dioximes may be observed.[13]

Figures 4 and 5 compare the dioxime profiles from the furan reactions with those from OH + aromatic experiments conducted at low extents of reaction. Assuming that the unsaturated 1,4-dicarbonyls formed from the OH + aromatic reactions are totally or almost totally in the *Z*-form (recognizing that some *Z*-/*E*-photoisomerization will occur, even for short irradiation times), it is obvious that 1,4-butenedial from the OH + furan reaction is formed dominantly as the *E*-isomer (Figure 4, traces 1A and 1B), 4-oxo-2-pentenal from OH + 2-methylfuran is mainly in the *E*-form (Figure 4, traces 2A and 2B), and 2-methyl-1,4-butenedial from OH + 3-methylfuran is formed in a *Z*-/*E*-mixture (Figure 5, traces 1A and 1B). 3-

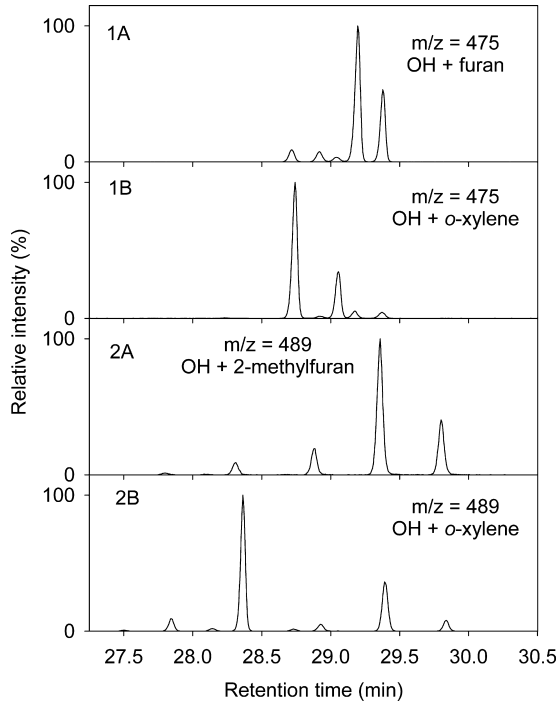

Figure 4. Positive chemical ionization GC−MS analyses of extracts of PFBHA-coated denuder samples collected after CH_3ONO−NO−air irradiations. 1A: m/z = 475 $[M+H]^+$ of dioximes of HC(O)CH=CHCHO from a furan reaction after 6 min irradiation; 1B: m/z = 475 $[M+H]^+$ of dioximes of HC(O)CH=CHCHO from an *o*-xylene reaction after 4 min irradiation; 2A: m/z = 489 $[M+H]^+$ of dioximes of $CH_3C(O)CH$=CHCHO from a 2-methylfuran reaction after 2 min irradiation; and 2B: m/z = 489 $[M+H]^+$ of dioximes of $CH_3C(O)$-CH=CHCHO from an *o*-xylene reaction after 4 min irradiation.

Methyl-4-oxo-2-pentenal from OH + 2,3-dimethylfuran also appears to be formed in a *Z*-/*E*-mixture (Figure 5, traces 2A and 2B), although this interpretation is less straightforward than for the furan and 2- and 3-methylfuran reactions. We previously found,[7] from GC−FID measurements of underivatized 3-hexene-2,5-dione, that in the presence of NO the OH + 2,5-dimethylfuran reaction forms 3-hexene-2,5-dione in the ratio 69 ± 4% *Z*/31 ± 4% *E*. In the presence of NO, there appears to be a gradual change from dominantly *E*-isomer formation of 1,4-butenedial from OH + furan to mainly *Z*-isomer formation of 3-hexene-2,5-dione from OH + 2,5-dimethylfuran. Our observation of mainly *E* unsaturated 1,4-dicarbonyl formation from OH + furan and 2-methylfuran is in agreement with the previous in situ Fourier transform infrared (FT-IR) spectral data of Bierbach et al.[5] for OH + furan and 2-methylfuran and the solid phase microextraction (SPME) fiber analyses of Gómez Alvarez et al.[6] for OH + furan.

Quantification of the Unsaturated 1,4-Dicarbonyls. *Concentrations Measured from Denuder Samples with Internal Standards.* Since unsaturated 1,4-dicarbonyls, other than diketones like 3-hexene-2,5-dione[7,11] and 3-methyl-3-hexene-2,5-dione,[14] do not appear to elute from GC columns without prior derivatization, the unsaturated 1,4-dicarbonyls were quantified as their dioximes. For the 3-methylfuran and 2,3-dimethylfuran reactions, minor amounts of mono-oximes were also observed and quantified. 2,5-Hexanedione was used as an internal standard, with its concentration in the chamber being measured by GC−FID analyses of samples collected onto Tenax solid adsorbent (without derivatization) and with it

dx.doi.org/10.1021/jp410345k | J. Phys. Chem. A 2014, 118, 457−466

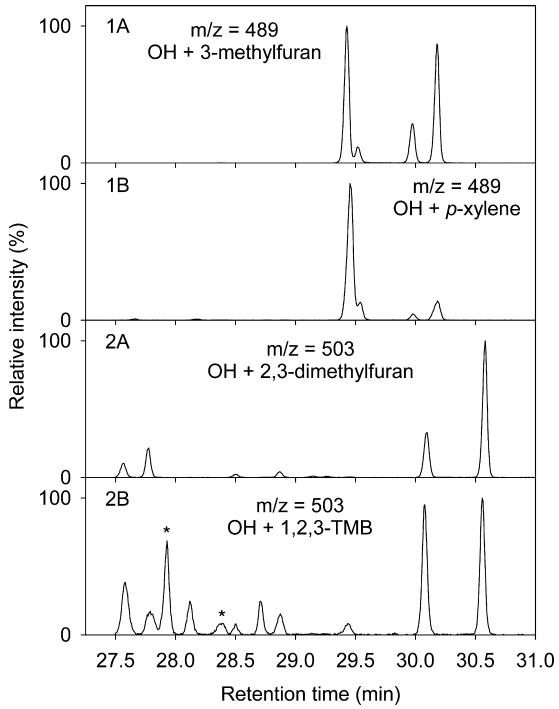

Figure 5. Positive chemical ionization GC−MS analyses of extracts of PFBHA-coated denuder samples collected after CH_3ONO−NO−air irradiations. 1A: m/z = 489 $[M+H]^+$ of dioximes of $HC(O)C(CH_3)$=CHCHO from a 3-methylfuran reaction after 4 min irradiation; 1B: m/z = 489 $[M+H]^+$ of dioximes of $HC(O)C(CH_3)$=CHCHO from a *p*-xylene reaction after 4 min irradiation; 2A: m/z = 503 $[M+H]^+$ of dioximes of $CH_3C(O)C(CH_3)$=CHCHO from a 2,3-dimethylfuran reaction after 3 min irradiation; and 2B: m/z = 503 $[M+H]^+$ of dioximes of $CH_3C(O)C(CH_3)$=CHCHO from a 1,2,3-trimethylbenzene (1,2,3-TMB) reaction after 2 min irradiation. The peaks labeled with asterisks in 2B are not due to $CH_3C(O)C(CH_3)$=CHCHO (the first asterisked peak being a m/z = 503 $[M+H-H_2O]^+$ of dioximes of a molecular weight 130 hydroxydicarbonyl, possibly $CH_3C(O)C(O)C(CH_3)(OH)C(O)CH_3$ or isomer formed as a second-generation product from OH + unsaturated 1,4-dicarbonyl). An additional ion peak must not be due to $CH_3C(O)C(CH_3)$=CHCHO, since a maximum of eight are expected.

being observed in the PFBHA-coated denuder samples as its dioximes (no mono-oximes of 2,5-hexanedione were observed). Hence by ratioing the GC−FID peaks areas of the oximes of the unsaturated 1,4-dicarbonyls to those of 2,5-hexanedione and taking into account the differing FID responses of the oximes of the unsaturated 1,4-dicarbonyls and of 2,5-hexanedione (using the Effective Carbon Numbers (ECNs) of Scanlon and Willis[22] and Nishino et al.[23]), the concentrations of the unsaturated dicarbonyls in the chamber could be derived.

As a check on this approach, the glyoxal formation yield from OH + 3-methyl-2-butenal was measured using this procedure. After correcting for the GC−FID responses of the dioximes of 2,5-hexanedione and glyoxal using their calculated ECNs,[22,23] and for reaction of glyoxal with OH radicals,[16] the glyoxal formation yield was determined to be 40 ± 5%, where the indicated error is two standard deviations of the four replicate analyses of the extract combined with estimated uncertainties in the GC−FID response factors for 3-methyl-2-butenal and 2,5-hexanedione of ±5% each. This formation yield is in excellent agreement with that of 40 ± 3% measured by Tuazon et al.[16] using in situ FT-IR spectroscopy, indicating that the collection and derivatization efficiencies of 2,5-hexanedione and glyoxal were essentially identical and that the use of the calculated ECNs was appropriate.

The before and after reaction concentrations of the furans and the after reaction concentrations of the unsaturated 1,4-dicarbonyls are listed in Table S1 (Supporting Information) (in parts-per-billion (ppbV) mixing ratio; 1 ppbV = 2.40×10^{10} molecules cm^{-3} for the temperature and total pressure conditions of this study). As evident from Table S1, up to five replicate postreaction GC−FID analyses of the extract of the PFBHA-coated denuder sample were conducted, with excellent reproducibility relative to the internal standard.

Corrections for Losses of Unsaturated 1,4-Dicarbonyls. The unsaturated 1,4-dicarbonyls also react with OH radicals and undergo photolysis, and these unsaturated dicarbonyl loss processes need to be taken into account in order to obtain their formation yields. For a given furan, the OH radical concentrations averaged over the irradiation period were independent of the irradiation time, with ≤13% change in the OH radical concentration for a factor of 2 change in the irradiation time (see the denuder samples in Table S2 (Supporting Information), for which the irradiation times were varied for identical initial CH_3ONO and NO concentrations). Hence the OH radical concentrations could be taken to be constant during an individual experiment, and corrections for secondary reactions were carried out as described previously,[24] with k(unsaturated 1,4-dicarbonyl)/k(furan) = k_2/k_1 = {k(OH + unsaturated 1,4-dicarbonyl)[OH] + k(photolysis of unsaturated 1,4-dicarbonyl) + k(wall loss of unsaturated 1,4-dicarbonyl)}/k(OH + furan)[OH], and with the correction factors depending on the ratio k_2/k_1 and the extent of reaction.[24]

Rate constants for the OH radical reactions of the *Z* and *E* unsaturated 1,4-dicarbonyls and their rates of photolysis by blacklamps are, however, not well-known. Rate constants have been measured for the reactions of OH radicals with 1,4-butenedial, 4-oxopentenal and 3-hexene-2,5-dione, with room temperature rate constants of (in units of 10^{-11} cm^3 $molecule^{-1}$ s^{-1}): *Z*-1,4-butenedial, 5.29 ± 0.11;[25,26] *E*-1,4-butenedial, 3.45 ± 0.34;[27] *Z*-/*E*-mixture of 4-oxo-2-pentenal, 5.67 ± 0.22;[25,26] *Z*-3-hexene-2,5-dione, 5.90 ± 0.57;[7] and *E*-3-hexene-2,5-dione, 4.14 ± 0.02.[7]

We obtained additional information concerning the rate ratios k_2/k_1 pertinent to our experiments by analyzing the time−concentration behavior of the unsaturated 1,4-dicarbonyls during OH radical-initiated reactions of the furans. This included additional experiments comprising continuous irradiations of CH_3ONO−NO−furan−air mixtures with analysis of the unsaturated 1,4-dicarbonyls every ∼3 min by API-MS. These data are presented and discussed in the Supporting Information, with Table S2 including data from the experiments with denuder sampling as well as from the additional experiments with API-MS analyses. On the basis of the available literature data concerning photolysis and reaction with OH radicals, and consistent with the values of k_2/k_1 obtained for unsaturated 1,4-dicarbonyl formation from our OH + furan reactions (see Supporting Information), we used rate constants for the OH radical reactions of (in units of 10^{-11} cm^3 $molecule^{-1}$ s^{-1}) of: *E*-1,4-butenedial, 3.45;[27] 4-oxo-2-pentenal, 5.67;[25,26] 2-methyl-1,4-butenedial and 3-methyl-4-oxo-2-pentenal, 6.0 each (estimated); and 3-hexene-2,5-dione, 5.35 (applicable for a 69% *Z*-/31% *E*-mixture[7]). A photolysis rate of J(unsaturated 1,4-dicarbonyl)/$J(NO_2)$ = 0.14 was used for

dx.doi.org/10.1021/jp410345k | J. Phys. Chem. A 2014, 118, 457−466

Table 2. Measured Formation Yields of Unsaturated 1,4-Dicarbonyls from the OH Radical-Initiated Reactions of Furans, Together with Literature Data

furan	unsaturated 1,4-dicarbonyl	molar yield (%)[a]	ref
furan	HC(O)CH=CHCHO	75 ± 5[b]	this work
		>70[c]	Bierbach et al.[5]
		109 ± 41[d]	Gómez Alvarez et al.[6]
		90 ± 36[d]	Gómez Alvarez et al.[6]
2-methylfuran	$CH_3C(O)CH=CHCHO$	31 ± 5[b]	this work
		~70[c]	Bierbach et al.[5]
		60 ± 24	Gómez Alvarez et al.[6]
3-methylfuran	$HC(O)C(CH_3)=CHCHO$	38 ± 2[b]	this work
		83 ± 33	Gómez Alvarez et al.[6]
		1.4 ± 0.3	Tapia et al.[8]
2,3-dimethylfuran	$CH_3C(O)C(CH_3)=CHCHO$	8 ± 2[b]	this work
2,5-dimethylfuran	$CH_3C(O)CH=CHC(O)CH_3$	27[e]	this work
		24 ± 3	Aschmann et al.[7]

[a]Experiments carried out in the presence of NO_x unless noted otherwise. In this work, analyses of the unsaturated 1,4-dicarbonyls was as their mono- (minor or not observed) and dioximes from GC−FID analyses of extracts of PFBHA-coated denuder samples (see text). [b]Indicated errors are two standard deviations and indicate precision only. [c]Experiments carried out in the absence of NO_x. [d]The two values are the HC(O)CH=CHCHO yields from each of two experiments conducted. [e]From a single experiment. Concurrent GC−FID analyses of samples collected onto Tenax solid adsorbent with subsequent thermal desorption resulted in a 3-hexene-2,5-dione yield of 22%.

1,4-butenedial and of 0.20 for 4-oxo-2-pentenal and 2-methyl-1,4-butenedial, based on the experimental data of Bierbach et al.[25] for *Z*- and *E*-1,4-butenedial and a *Z*-/*E*-mixture of 4-oxo-2-pentenal and of Thüner et al.[28] for *E*-1,4-butenedial and *Z*-4-oxo-2-pentenal. For our experimental conditions, photolysis was a minor fraction (14−22%) of the OH radical reaction rate for 1,4-butenedial, 4-oxo-2-pentenal, and 2-methyl-1,4-butenedial formed in the furan and 2- and 3-methylfuran reactions. Photolysis (other than photoisomerization) of 3-hexene-2,5-dione by black lamps is not important[7,11] and this was also assumed to be the case for 3-methyl-4-oxo-2-pentenal.

The use of these photolysis rates and OH radical reaction rate constants for the unsaturated 1,4-dicarbonyls, combined with OH radical reaction rate constants for the furans,[7] resulted in ratios k_2/k_1 of 1.02−1.04 for formation of 1,4-butenedial (predominantly the *E*-isomer) from OH + furan, 0.899−0.914 for formation of 4-oxo-2-pentenal from OH + 2-methylfuran, 0.783−0.792 for formation of 2-methyl-1,4-butenedial from OH + 3-methylfuran, 0.476 for formation of 3-methyl-4-oxo-2-pentenal from OH + 2,3-dimethylfuran, and 0.428 for formation of 3-hexene-2,5-dione from OH + 2,5-dimethylfuran, where the ranges for the furan and 2- and 3-methylfuran reactions are due to the varying importance of photolysis versus OH radical reaction of the unsaturated 1,4-dicarbonyl formed in the individual denuder experiments (Table S2, Supporting Information). The use of these k_2/k_1 ratios to correct for secondary reactions resulted in unsaturated 1,4-dicarbonyl formation yields which showed no obvious trend with extent of reaction, and therefore indicating that these values of k_2/k_1 were reasonable (see also Figures S5−S8 and the associated text in the Supporting Information). The resulting unsaturated 1,4-dicarbonyl formation yields are listed in Table 2. Note that in the single OH + 2,5-dimethylfuran experiment, 3-hexene-2,5-dione was also quantified from GC−FID analyses of samples collected onto Tenax solid adsorbent, with agreement to within 20% between analyses of 3-hexene-2,5-dione analyses from Tenax samples (without derivatization) and as its dioximes from extracts of PFBHA-coated denuder samples (Table 2).

The multiplicative correction factors[24] to account for losses of the unsaturated 1,4-dicarbonyls were 1.28−1.63 for 1,4-butenedial formation from OH + furan, 1.25−1.40 for 4-oxo-2-pentenal formation from OH + 2-methylfuran, 1.27−1.43 for 2-methyl-1,4-butenedial formation from OH + 3-methylfuran, 1.23−1.32 for 3-methyl-4-oxo-2-pentenal formation from OH + 2,3-dimethylfuran, and 1.10 for 3-hexene-2,5-dione formation from the single OH + 2,5-dimethylfuran reaction. While there are significant uncertainties in the k_2/k_1 ratios, especially for the formation of 4-oxo-2-pentenal from OH + 2-methylfuran, 2-methyl-1,4-butenedial from OH + 3-methylfuran, and 3-methyl-4-oxo-2-pentenal from OH + 2,3-dimethylfuran, only for formation of 1,4-butenedial from OH + furan would significant uncertainties in k_2/k_1 translate into significant uncertainties in the multiplicative correction factors (a ± 25% uncertainty in k_2/k_1 would result in uncertainties in the multiplicative correction factors of <10% for all but 1,4-butenedial from OH + furan). During the experiments, the denuder samples were collected over a period of 1.5 h, and the consistency of the k_2/k_1 ratios that fit the experimental data with measured[25−27] or estimated rate constants for the reactions of OH radicals with unsaturated 1,4-dicarbonyls indicates that their loss rates during our experiments were controlled mainly by reaction with OH radicals, and that losses to the chamber walls were minor and that photolysis was consistent with the literature data and of relatively minor importance. That wall losses were minor was confirmed by the preliminary experiments with 2,3-dimethylfuran, with yields obtained in experiments where PFBHA-coated denuder sampling was conducted 45 and 156 min after the irradiation period, being in good agreement with those where sampling was initiated immediately after the irradiation period (Table S1, Supporting Information), and by the additional experiments with in situ analyses of the unsaturated 1,4-dicarbonyls by API-MS (see, for example, Figures S9 and S10, Supporting Information).

Comparison with Literature Data. Previous literature unsaturated 1,4-dicarbonyl formation yields are listed in Table 2. Bierbach et al.[5] used in situ FT-IR spectroscopy to investigate the reactions of OH radicals with furan and 2-methylfuran in the absence of NO_x. The major products observed were 1,4-butenedial from furan and 4-oxo-2-pentenal from 2-methylfur-

dx.doi.org/10.1021/jp410345k | J. Phys. Chem. A 2014, 118, 457−466

an. Because of a lack of authentic standards, the absorption cross-section of the ~1720 cm^{-1} C=O stretch in 3-hexene-2,5-dione measured by Tuazon et al.[29] was used for quantification of 1,4-butenedial and 4-oxo-2-pentenal. Gómez Alvarez et al.[6] used SPME with on-fiber derivatization and GC−FID to quantify the unsaturated 1,4-dicarbonyls as their oximes from the furan and 2- and 3-methylfuran reactions, with calibration of *E*-1,4-butenedial by use of a synthesized standard. The SPME GC−FID response factor for *E*-1,4-butenedial was used for the quantification of *Z*-1,4-butenedial and the *Z*- and *E*-isomers of 4-oxo-2-pentenal and 2-methyl-1,4-butenedial.

Tapia et al.[8] observed the formation of acetic acid, 3-furaldehyde (3-furancarboxaldehyde), 2-methyl-1,4-butenedial, 3-methyl-2,5-furandione, 3-methyl-2(3*H*)-furanone and 2-hydroxy-3-methyl-5-(2*H*)-furanone from the OH radical-initiated reaction of 3-methylfuran in the presence of NO, using photolysis of CH_3ONO at 254 and 360 nm in a 150 L Teflon-coated chamber with samples being collected onto SPME fibers without derivatization and with GC−MS analyses. The reported molar yields, uncorrected for secondary reactions, were 3.9 ± 1.8% for 3-furaldehyde, 1.4 ± 0.3% for 2-methyl-1,4-butenedial, 18.1 ± 4.6% for 3-methyl-2,5-furandione, and 1.6 ± 0.2% for 3-methyl-2(3*H*)-furanone.[8] While the much lower yield of 2-methyl-1,4-butenedial reported by Tapia et al.,[8] using SPME without derivatization, than measured by Gómez Alvarez et al.,[6] using SPME fibers with on-fiber derivatization, was ascribed to potentially fast secondary loss processes,[8] we have not been able to quantitatively analyze unsaturated 1,4-dicarbonyls by gas chromatography without prior derivatization, presumably due to adsorption and/or polymerization on the sampling and/or chromatographic column surfaces. Hence it is likely that the very low yield of 2-methyl-1,4-butenedial in the Tapia et al.[8] study was due to analytical problems.

Apart from the quantification of *E*-1,4-butenedial from OH + furan by Gómez Alvarez et al.,[6] the other literature yield measurements[5,6,8] are subject to analytical uncertainties[8] or uncertainties in the FT-IR absorption cross sections[5] or in the SPME GC−FID response factors,[6] which include the on-fiber collection and derivatization efficiency which can vary significantly.[30] Our 1,4-butenedial yield from OH + furan in the presence of NO agrees well with those of Bierbach et al.[5] (in the absence of NO) and Gómez Alvarez et al.[6] All three studies show that formation of 1,4-butenedial dominates, and that 1,4-butenedial is formed primarily in the *E*-configuration, with Gómez Alvarez et al.[6] finding a 76% *E*-/24% *Z*-isomer distribution. For OH + 2-methylfuran and OH + 3-methylfuran, our measured 4-oxo-2-pentenal and 2-methyl-1,4-butenedial formation yields are lower by a factor of ~2 than those reported by Bierbach et al.[5] for OH + 2-methylfuran (in the absence of NO) and Gómez Alvarez et al.[6] for 2- and 3-methylfuran (in the presence of NO). While the previous studies did not differentiate the *Z*-/*E*-isomer composition of the unsaturated 1,4-dicarbonyls formed in the 2- and 3-methylfuran reactions, we find that 4-oxo-2-pentenal formed from 2-methylfuran is primarily in the *E*-configuration, while 2-methyl-1,4-butenedial from 3-methylfuran is a *Z*-/*E*-mixture.

It is apparent from Table 2 that our unsaturated 1,4-dicarbonyl formation yields decrease markedly from 75 ± 5% for the furan reaction to 8 ± 2% for the 2,3-dimethylfuran reaction and, as noted above and in Table 2, our 4-oxo-2-pentenal and 2-methyl-1,4-butenedial yields from 2- and 3-methylfuran, respectively, are a factor of ~2 lower than those of Bierbach et al.[5] and Gómez Alvarez et al.[6] The present study and that of Gómez Alvarez et al.[6] were carried out in the presence of NO, while that of Bierbach et al.[5] was in the absence of NO. Note that pathway (B) in Scheme 1 as written would only occur in the presence of NO, and hence a higher yield of unsaturated 1,4-dicarbonyl would be expected in the absence of NO then in the presence of NO, as we observed for 3-hexene-2,5-dione formation from OH + 2,5-dimethylfuran,[7] with 3-hexene-2,5-dione yields of 34 ± 3% in the absence of NO and 24 ± 3% in the presence of NO. Hence the unsaturated 1,4-dicarbonyl yields from the OH + furan, 2- and 3-methylfuran and 2,3-dimethylfuran reactions in the absence of NO are also likely to be higher than those measured in the presence of NO.

The unsaturated 1,4-dicarbonyl formation yields measured in this study could be low because of (a) less than 100% collection and derivatization efficiency for the C_5 and C_6 unsaturated 1,4-dicarbonyls, (b) rapid losses of the unsaturated 1,4-dicarbonyls to the chamber walls or to aerosol (noting that Gómez Alvarez et al.[6] measured aerosol yields from 2- and 3-methylfuran of <6%), (c) rapid photolysis of the unsaturated 1,4-dicarbonyls, or (d) partitioning of the unsaturated 1,4-dicarbonyls to the chamber walls with an equilibrium being attained. Our discussion above showing no evidence for significant wall losses of 3-methyl-4-oxo-2-pentenal from experiments in which sampling was initiated up to 156 min after the irradiation period compared to sampling immediately after the irradiation period argues against possibility (b). The fact that the variation of measured unsaturated 1,4-dicarbonyl concentration with extent of reaction (Figures S5−S8, Supporting Information) shows no evidence for unsaturated 1,4-dicarbonyl loss rates greater than expected from OH radical reaction plus a small contribution from photolysis argues against possibilities (b) and (c). For a given carbon number, aldehydes derivatize more easily than ketones,[15,30] and hence 3-hexene-2,5-dione would be expected to be the slowest to derivatize. However, the 3-hexene-2,5-dione formation yield from the OH + 2,5-dimethylfuran reaction as measured using the PFBHA-coated denuder procedure is in good agreement with the yield we previously measured[7] from samples collected onto Tenax solid adsorbent with subsequent thermal desorption and GC−FID analysis (without derivatization). We have also shown that the collection and derivatization efficiencies of 2,5-hexanedione, 5-methyl-2-hexanone, 2-octanone, and 2-decanone on PFBHA-coated denuders are equal to within 10%.[21] This argues against possibility (a), although mono-oximes were observed for 2-methyl-1,4-butenedial from 3-methylfuran and for 3-methyl-4-oxo-2-pentenal from 2,3-dimethylfuran, with the dioximes accounting for ≥94% of the total oximes for 2-methyl-1,4-butenedial from 3-methylfuran and for ≥75% of the total oximes for 3-methyl-4-oxo-2-pentenal from 2,3-dimethylfuran (but only 44−63% of the total oximes in the three preliminary experiments which, however, gave results in good agreement with the subsequent four experiments (see Table S1, Supporting Information)).

Finally, to investigate the possibility of significant equilibrium partitioning to the chamber walls, two experiments were carried out for OH + 2,3-dimethylfuran, with 2,5-hexanedione present, in which PFBHA-coated denuder samples were collected immediately after a single irradiation period and after the chamber was emptied and backfilled with dry purified air (a total period of 2.15−2.55 h elapsing between the two denuder samples). The chamber contents were diluted by factors of 4.2 ± 0.4 and 14 ± 3 in the two experiments. Hence, if 3-methyl-4-

dx.doi.org/10.1021/jp410345k | J. Phys. Chem. A 2014, 118, 457−466

oxo-2-pentenal had partitioned mainly to the chamber walls with an equilibrium being set up between gas- and wall-phase, then the (3-methyl-4-oxo-2-pentenal dioximes/2,5-hexanedione dioximes) ratio would increase from the first denuder sample to the second denuder sample in the two experiments by factors of up to 4 and 14, respectively, assuming that no such partitioning of 2,5-hexanedione occurs. The (3-methyl-4-oxo-2-pentenal dioximes/2,5-hexanedione dioximes) ratio after the dilution and backfilling compared to that directly after the irradiation was 1.5 in the first experiment (versus up to 4.2 expected) and 0.6 in the second experiment (versus up to 14 expected). While the GC−FID signals after the chamber was emptied and backfilled were low, these two experiments show no clear evidence for significant off-gassing of 3-methyl-4-oxo-2-pentenal from the chamber walls, and hence argue against possibility (d).

Unsaturated 1,4-dicarbonyls, and 1,2-dicarbonyls, are also formed from the OH radical-initiated reactions of monocyclic aromatic hydrocarbons.[9−14,23,26,31−33] Glyoxal, methylglyoxal and 2,3-butanedione formation yields from the toluene, *o*-, *m*- and *p*-xylene, and 1,2,3-, 1,2,4- and 1,3,5-trimethylbenzene reactions have been obtained at low NO_2 concentrations by Atkinson and Aschmann,[33] Bethel et al.[11] and Nishino et al.[23] The 3-hexene-2,5-dione formation yields of Bethel et al.[11] from the OH + *p*-xylene and OH + 1,2,4-trimethylbenzene reactions are identical, within the experimental uncertainties, with the coproduct glyoxal[23,32] and methylglyoxal[23] formation yields, respectively. As discussed and presented in the Supporting Information, using the same analytical procedures as employed here, the measured formation yields of 1,4-butenedial[13] are similar to those of its assumed coproducts[23,33] from the OH + toluene and OH + *o*-xylene reactions (Tables S3 and S4 and Figure S12, Supporting Information). However, the formation yields of 4-oxo-2-pentenal, 2-methyl-1,4-butenedial, and 3-methyl-4-oxo-2-pentenal are significantly lower than those of their assumed coproducts (Tables S3 and S4 and Figure S12, Supporting Information).[13] These observations suggest that, for whatever reason (but not including more rapid losses from the gas-phase than anticipated), the amounts of 4-oxo-2-pentenal, 2-methyl-1,4-butenedial and 3-methyl-4-oxo-2-pentenal produced in the OH radical-initiated reactions of methyl-substituted benzenes are not quantitatively observed. The OH + aromatics data suggest that our measured formation yields of 4-oxo-2-pentenal, 2-methyl-1,4-butenedial, and 3-methyl-4-oxo-2-pentenal from 2-methylfuran, 3-methylfuran and 2,3-dimethylfuran could be low. One possibility not considered above is that some or most of the unsaturated 1,4-dialdehydes (other than 1,4-butenedial) and unsaturated 1,4-keto-aldehydes (which do not appear to elute from GC columns without prior derivatization) undergo heterogeneous reactions (possibly oligomer formation) on the denuder and other surfaces (but obviously not rapidly on Teflon film), or are in equilibrium with an isomer which was not observed in our previous study of OH + aromatic reactions nor in the present study. However, it is quite obvious that other products are also formed from the OH + furan reactions; indeed, in the presence of NO the yield of 3-hexene-2,5-dione from OH + 2,5-dimethylfuran is only 24 ± 3% (Table 2).[7] While it is possible that our measured formation yields of 4-oxo-2-pentenal from OH + 2-methylfuran, 2-methyl-1,4-butenedial from OH + 3-methylfuran, and 3-methyl-4-oxo-2-pentenal from OH + 2,3-dimethylfuran are low (and this would be more consistent with unsaturated 1,4-dicarbonyls being coproducts to the observed 1,2-dicarbonyls in OH + aromatic hydrocarbon reactions), we have no evidence of problems which would lead to erroneously low formation yields for these specific unsaturated 1,4-dicarbonyls in this study.

Theoretical studies of the reactions of OH radicals with furan,[34] 2-methylfuran,[35,36] and 3-methylfuran[37] all conclude that the dominant pathway at room temperature involves OH radical addition at the 2- or 5-positions, to form RC(O)CR′=CHC$^{\bullet}$HOH and/or RC$^{\bullet}$(OH)CR′=CHCHO, where R and R′ are H and H for furan, CH_3 and H for 2-methylfuran, and H and CH_3 for 3-methylfuran (i.e., to form the α-hydroxy radical product involved in pathways A and B in Scheme 1). Our experimental data indicate that additional reaction pathways are involved leading to additional products and suggest that these are especially significant for 2,3- and 2,5-dimethylfuran. Very recently, Davis and Sarathy[36] have carried out a computational study of potential reactions occurring subsequent to O_2 reaction with the radicals formed by OH addition to 2-methylfuran in the absence of NO.

■ ASSOCIATED CONTENT

Supporting Information

Twenty five pages of Supporting Information are available, comprising Tables S1−S4, Figures S1−S12, and discussion of the time−concentration behavior of unsaturated 1,4-dicarbonyls during OH + furan reactions and of formation of unsaturated 1,4-dicarbonyls and 1,2-dicarbonyls from OH + aromatic hydrocarbon reactions. This information is available free of charge via the Internet, at http://pubs.acs.org/.

■ AUTHOR INFORMATION

Corresponding Authors

*J.A.: e-mail, janet.arey@ucr.edu; telephone, 951 452-4502.

*R.A.: e-mail, ratkins@mail.ucr.edu; telephone, 951 452-4503.

Present Addresses

[†]Department of Chemistry, University of California, Irvine, CA 92697.

[‡]Also Department of Environmental Sciences, University of California, Riverside, CA 92521.

Notes

The authors declare no competing financial interest.

■ ACKNOWLEDGMENTS

The authors thank the U.S. Environmental Protection Agency (Grant No. R833752) for supporting this research. While this work has been supported by this Agency, the results and the contents of this publication do not necessarily reflect the views and the opinions of the Agency. J.A. thanks the University of California Agricultural Experiment Station for partial salary support.

■ REFERENCES

(1) Graedel, T. E.; Hawkins, D. T.; Claxton, L. D. *Atmospheric Chemical Compounds: Sources, Occurrence and Bioassay*; Academic Press: New York, 1986.

(2) Ciccioli, P.; Brancaleoni, E.; Frattoni, M.; Cecinato, A.; Pinciarelli, L. Determination of Volatile Organic Compounds (VOC) Emitted from Biomass Burning of Mediterranean Vegetation Species by GC-MS. *Anal. Lett.* **2001**, *34*, 937−955.

(3) Andreae, M. O.; Merlet, P. Emission of Trace Gases and Aerosols from Biomass Burning. *Global Biogeochem. Cycles* **2001**, *15*, 955−966.

(4) Atkinson, R.; Arey, J. Atmospheric Degradation of Volatile Organic Compounds. *Chem. Rev.* **2003**, *103*, 4605−4638.

(5) Bierbach, A.; Barnes, I.; Becker, K. H. Product and Kinetic Study of the OH-Initiated Gas-Phase Oxidation of Furan, 2-Methylfuran and Furanaldehydes at ≈300 K. *Atmos. Environ.* **1995**, *29*, 2651−2660.
(6) Gómez Alvarez, E.; Borrás, E.; Viidanoja, J.; Hjorth, J. Unsaturated Dicarbonyl Products from the OH-Initiated Photooxidation of Furan, 2-Methylfuran and 3-Methylfuran. *Atmos. Environ.* **2009**, *43*, 1603−1612.
(7) Aschmann, S. M.; Nishino, N.; Arey, J.; Atkinson, R. Kinetics of the Reactions of OH Radicals with 2- and 3-Methylfuran, 2,3- and 2,5-Dimethylfuran, and *E*- and *Z*-3-Hexene-2,5-dione, and Products of OH + 2,5-Dimethylfuran. *Environ. Sci. Technol.* **2011**, *45*, 1859−1865.
(8) Tapia, A.; Villanueva, F.; Salgado, M. S.; Cabañas, B.; Martinez, E.; Martin, P. Atmospheric Degradation of 3-Methylfuran: Kinetics and Products Study. *Atmos. Chem. Phys.* **2011**, *11*, 3227−3241.
(9) Smith, D. F.; McIver, C. D.; Kleindienst, T. E. Primary Product Distribution from the Reaction of Hydroxyl Radicals with Toluene at ppb NO_x Mixing Ratios. *J. Atmos. Chem.* **1998**, *30*, 209−228.
(10) Smith, D. F.; Kleindienst, T. E.; McIver, C. D. Primary Product Distributions from the Reaction of OH with *m*-, *p*-Xylene, 1,2,4- and 1,3,5-Trimethylbenzene. *J. Atmos. Chem.* **1999**, *34*, 339−364.
(11) Bethel, H. L.; Atkinson, R.; Arey, J. Products of the Gas-Phase Reactions of OH Radicals with *p*-Xylene and 1,2,3- and 1,2,4-Trimethylbenzene: Effect of NO_2 Concentration. *J. Phys. Chem. A* **2000**, *104*, 8922−8929.
(12) Gómez Alvarez, E.; Viidanoja, J.; Muñoz, A.; Wirtz, K.; Hjorth, J. Experimental Confirmation of the Dicarbonyl Route in the Photo-Oxidation of Toluene and Benzene. *Environ. Sci. Technol.* **2007**, *41*, 8362−8369.
(13) Arey, J.; Obermeyer, G.; Aschmann, S. M.; Chattopadhyay, S.; Cusick, R. D.; Atkinson, R. Dicarbonyl Products of the OH Radical-Initiated Reaction of a Series of Aromatic Hydrocarbons. *Environ. Sci. Technol.* **2009**, *43*, 683−689.
(14) Aschmann, S. M.; Arey, J.; Atkinson, R. Rate Constants for the Reactions of OH Radicals with 1,2,4,5-Tetramethylbenzene, Pentamethylbenzene, 2,4,5-Trimethylbenzaldehyde, 2,4,5-Trimethylphenol, and 3-Methyl-3-hexene-2,5-dione and Products of OH + 1,2,4,5-Tetramethylbenzene. *J. Phys. Chem. A* **2013**, *117*, 2556−2568.
(15) Temime, B.; Healy, R. M.; Wenger, J. C. A Denuder-Filter Sampling Technique for the Detection of Gas and Particle Phase Carbonyl Compounds. *Environ. Sci. Technol.* **2007**, *41*, 6514−6520.
(16) Tuazon, E. C.; Aschmann, S. M.; Nishino, N.; Arey, J.; Atkinson, R. Kinetics and Products of the OH Radical-Initiated Reaction of 3-Methyl-2-butenal. *Phys. Chem. Chem. Phys.* **2005**, *7*, 2298−2304.
(17) Arey, J.; Aschmann, S. M.; Kwok, E. S. C.; Atkinson, R. Alkyl Nitrate, Hydroxyalkyl Nitrate, and Hydroxycarbonyl Formation from the NO_x-Air Photooxidations of C_5-C_8 *n*-Alkanes. *J. Phys. Chem. A* **2001**, *105*, 1020−1027.
(18) Taylor, W. D.; Allston, T. D.; Moscato, M. J.; Fazekas, G. B.; Kozlowski, R.; Takacs, G. A. Atmospheric Photodissociation Lifetimes for Nitromethane, Methyl Nitrite, and Methyl Nitrate. *Int. J. Chem. Kinet.* **1980**, *12*, 231−240.
(19) Dagaut, P.; Wallington, T. J.; Liu, R.; Kurylo, M. J. A Kinetic Investigation of the Gas-Phase Reactions of OH Radicals with Cyclic Ketones and Diones: Mechanistic Insights. *J. Phys. Chem.* **1988**, *92*, 4375−4377.
(20) Obermeyer, G.; Aschmann, S. M.; Atkinson, R.; Arey, J. Carbonyl Atmospheric Reaction Products of Aromatic Hydrocarbons in Ambient Air. *Atmos. Environ.* **2009**, *43*, 3736−3744.
(21) Aschmann, S. M.; Arey, J.; Atkinson, R. Reaction of OH Radicals with 5-Hydroxy-2-pentanone: Formation of 4-Oxopentanal and its OH Radical Reaction Rate Constant. *Environ. Chem.* **2013**, *10*, 145−150.
(22) Scanlon, J. T.; Willis, D. E. Calculation of Flame Ionization Detector Relative Response Factors using the Effective Carbon Number Concept. *J. Chromat. Sci.* **1985**, *23*, 333−340.
(23) Nishino, N.; Arey, J.; Atkinson, R. Formation Yields of Glyoxal and Methylglyoxal from the Gas-Phase OH Radical-Initiated Reactions of Toluene, Xylenes, and Trimethylbenzenes as a Function of NO_2 Concentration. *J. Phys. Chem. A* **2010**, *114*, 10140−10147.
(24) Atkinson, R.; Aschmann, S. M.; Carter, W. P. L.; Winer, A. M.; Pitts, J. N., Jr. Alkyl Nitrate Formation from the NO_x−Air Photooxidations of C_2-C_8 *n*-Alkanes. *J. Phys. Chem.* **1982**, *86*, 4563−4569.
(25) Bierbach, A.; Barnes, I.; Becker, K. H.; Wiesen, E. Atmospheric Chemistry of Unsaturated Carbonyls: Butenedial, 4-Oxo-2-pentenal, 3-Hexene-2,5-dione, Maleic Anhydride, 3*H*-Furan-2-one, and 5-Methyl-3*H*-furan-2-one. *Environ. Sci. Technol.* **1994**, *28*, 715−729.
(26) Calvert, J. G.; Atkinson, R.; Becker, K. H.; Kamens, R. M.; Seinfeld, J. H.; Wallington, T. J.; Yarwood, G. *The Mechanisms of Atmospheric Oxidation of Aromatic Hydrocarbons*, Oxford University Press, New York, 2002.
(27) Martín, P.; Cabañas, B.; Colmenar, I.; Salgado, M. S.; Villanueva, F.; Tapia, A. Reactivity of *E*-Butenedial with the Major Atmospheric Oxidants. *Atmos. Environ.* **2013**, *70*, 351−360.
(28) Thüner, L. P.; Rea, G.; Wenger, J. C. *Photolysis of Butenedial and 4-Oxopent-2-enal*. The European Photoreactor EUPHORE, 4th Report 2001, Barnes, I. (ed), Institute of Physical Chemistry, Bergische Universität Wuppertal, Wuppertal, Germany, November 2003, pp 41−46.
(29) Tuazon, E. C.; Atkinson, R.; Carter, W. P. L. Atmospheric Chemistry of *cis*- and *trans*-3-Hexene-2,5-dione. *Environ. Sci. Technol.* **1985**, *19*, 265−269.
(30) Reisen, F.; Aschmann, S. M.; Atkinson, R.; Arey, J. Hydroxyaldehyde Products from Hydroxyl Radical Reactions of *Z*-3-Hexen-1-ol and 2-Methyl-3-buten-2-ol Quantified by SPME and API-MS. *Environ. Sci. Technol.* **2003**, *37*, 4664−4671.
(31) Volkamer, R.; Platt, U.; Wirtz, K. Primary and Secondary Glyoxal Formation from Aromatics: Experimental Evidence for the Bicycloalkyl-Radical Pathway from Benzene, Toluene, and *p*-Xylene. *J. Phys. Chem. A* **2001**, *105*, 7865−7874.
(32) Volkamer, R.; Spietz, P.; Burrows, J.; Platt, U. High-Resolution Absorption Cross-Section of Glyoxal in the UV-Vis and IR Spectral Ranges. *J. Photochem. Photobiol. A: Chem.* **2005**, *172*, 35−46.
(33) Atkinson, R.; Aschmann, S. M. Products of the Gas-Phase Reactions of Aromatic Hydrocarbons: Effect of NO_2 Concentration. *Int. J. Chem. Kinet.* **1994**, *26*, 929−944.
(34) Mousavipour, S. H.; Ramazani, S.; Shahkolahi, Z. Multichannel RRKM-TST and Direct-Dynamics VTST Study of the Reaction of Hydroxyl Radical with Furan. *J. Phys. Chem. A* **2009**, *113*, 2838−2846.
(35) Zhang, W.; Du, B.; Mu, L.; Feng, C. Computational Study on the Mechanism for the Reaction of OH with 2-Methylfuran. *THEOCHEM* **2008**, *851*, 353−357.
(36) Davis, A. C.; Sarathy, S. M. Computational Study of the Combustion and Atmospheric Decomposition of 2-Methylfuran. *J. Phys. Chem. A* **2013**, *117*, 7670−7685.
(37) Zhang, W.; Du, B.; Mu, L.; Feng, C. Mechanism for the Gas-Phase Reaction between OH and 3-Methylfuran: A Theoretical Study. *Int. J. Quantum Chem.* **2008**, *108*, 1232−1238.

Supporting Information

to

Products of the OH Radical-Initiated Reactions of Furan, 2- and 3-Methylfuran, and 2,3- and 2,5-Dimethylfuran in the Presence of NO

Sara M. Aschmann, Noriko Nishino, Janet Arey* and Roger Atkinson*

Air Pollution Research Center

University of California

Riverside, CA 92521

Pages: 25

Tables: 4

Figures: 12

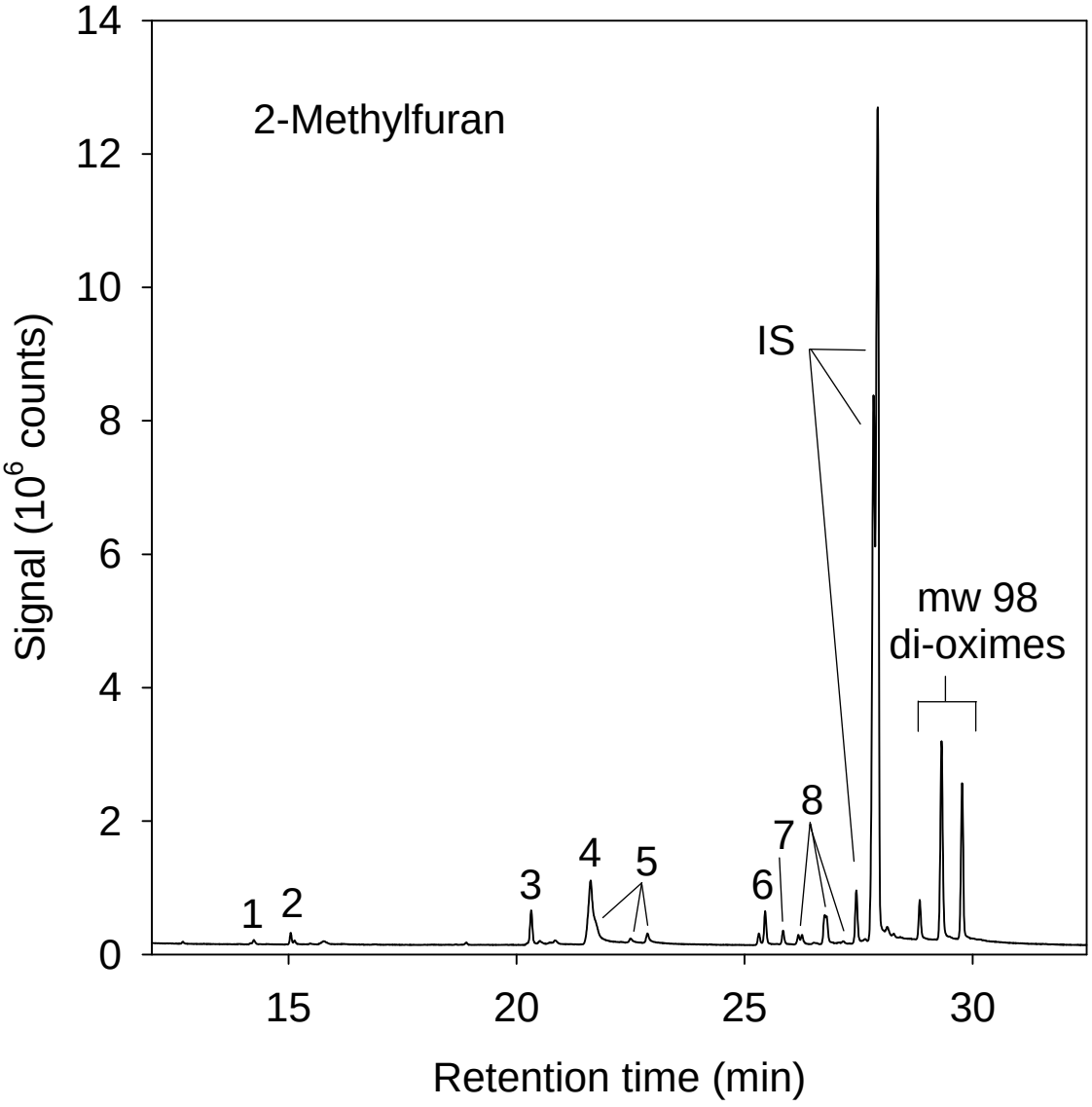

Figure S1. Positive chemical ionization GC-MS total ion chromatogram (TIC) of an extract of a PFBHA-coated denuder sample collected after 2.5 min irradiation of a CH_3ONO – NO – 2-methylfuran – 2,5-hexanedione (internal standard, IS) – air mixture, with 41% consumption of the initially present 2-methylfuran. IS = di-oximes of 2,5-hexanedione, the internal standard; peak #1, mono-oxime of molecular weight (mw) 72 dicarbonyl; peak #2, mono-oxime of $CH_3C(O)CH_2CHO$ (mw 86) formed from OH + 2,5-hexanedione; peaks #3, from derivatizing agent; peak #4, mono-oxime of mw 100 carbonyl; peaks #5, mono-oximes of mw 114 carbonyl; peaks #6, di-oximes of glyoxal; peak #7, di-oxime of methylglyoxal (mw 72); peaks #8, di-oximes of $CH_3C(O)CH_2CHO$ formed from OH + 2,5-hexanedione; and mw 98 di-oximes attributed to $CH_3C(O)CH=CHCHO$.

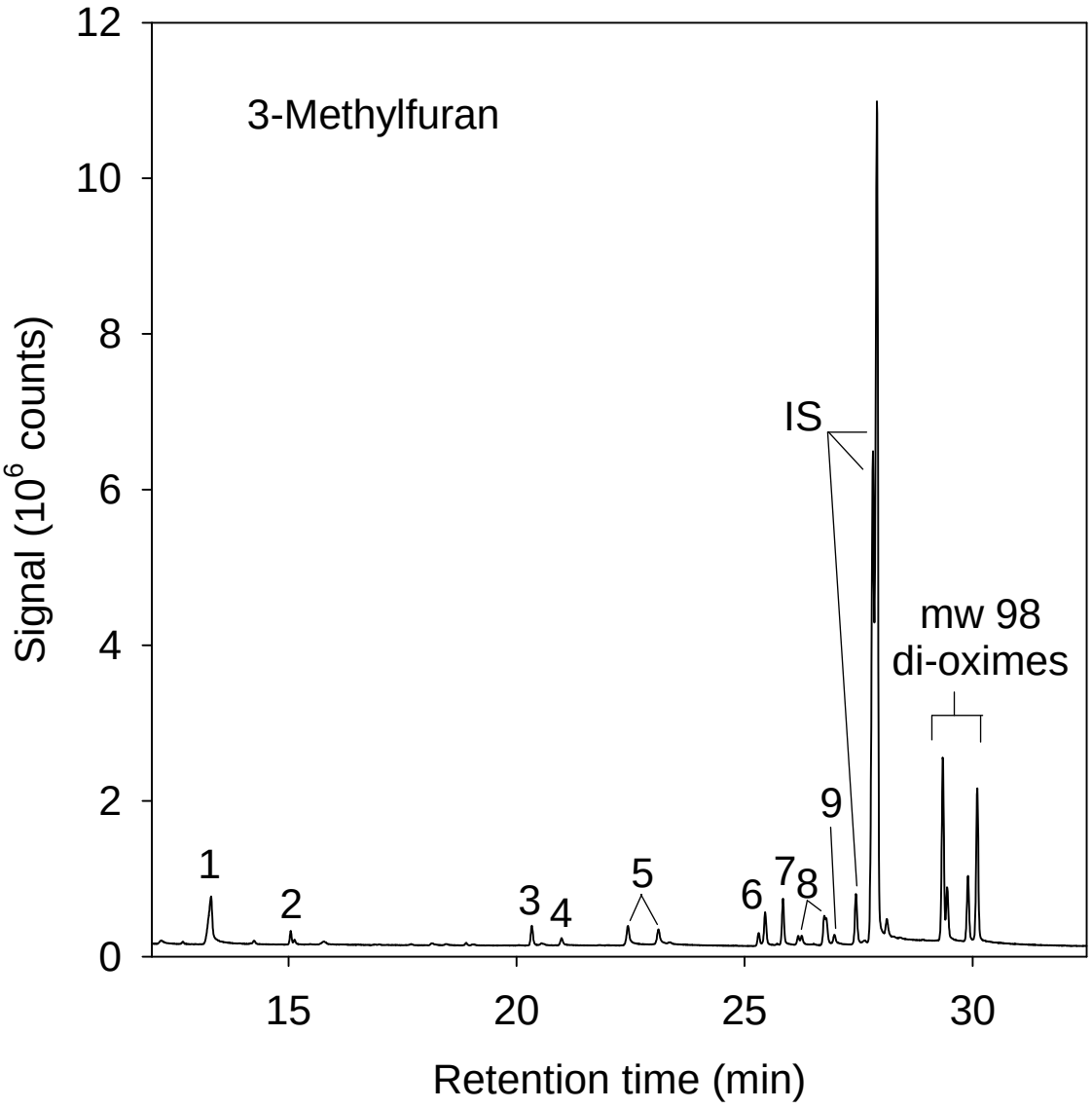

Figure S2. Positive chemical ionization GC-MS total ion chromatogram (TIC) of an extract of a PFBHA-coated denuder sample collected after 4 min irradiation of a CH_3ONO – NO – 3-methylfuran – 2,5-hexanedione (internal standard, IS) – air mixture, with 46% consumption of the initially present 3-methylfuran. IS = di-oximes of 2,5-hexanedione, the internal standard; peak #1, ions at m/z 115 and 97 present; peak #2, mono-oxime of $CH_3C(O)CH_2CHO$ (mw 86) formed from OH + 2,5-hexanedione; peak #3, from derivatizing agent; peak #4, mono-oxime of mw 98 dicarbonyl; peaks #5, mono-oximes of mw 114 carbonyl; peaks #6, di-oximes of glyoxal; peak #7, di-oxime of methylglyoxal (mw 72); peaks #8, di-oximes of $CH_3C(O)CH_2CHO$ formed from OH + 2,5-hexanedione; and mw 98 di-oximes attributed to $HC(O)C(CH_3)=CHCHO$.

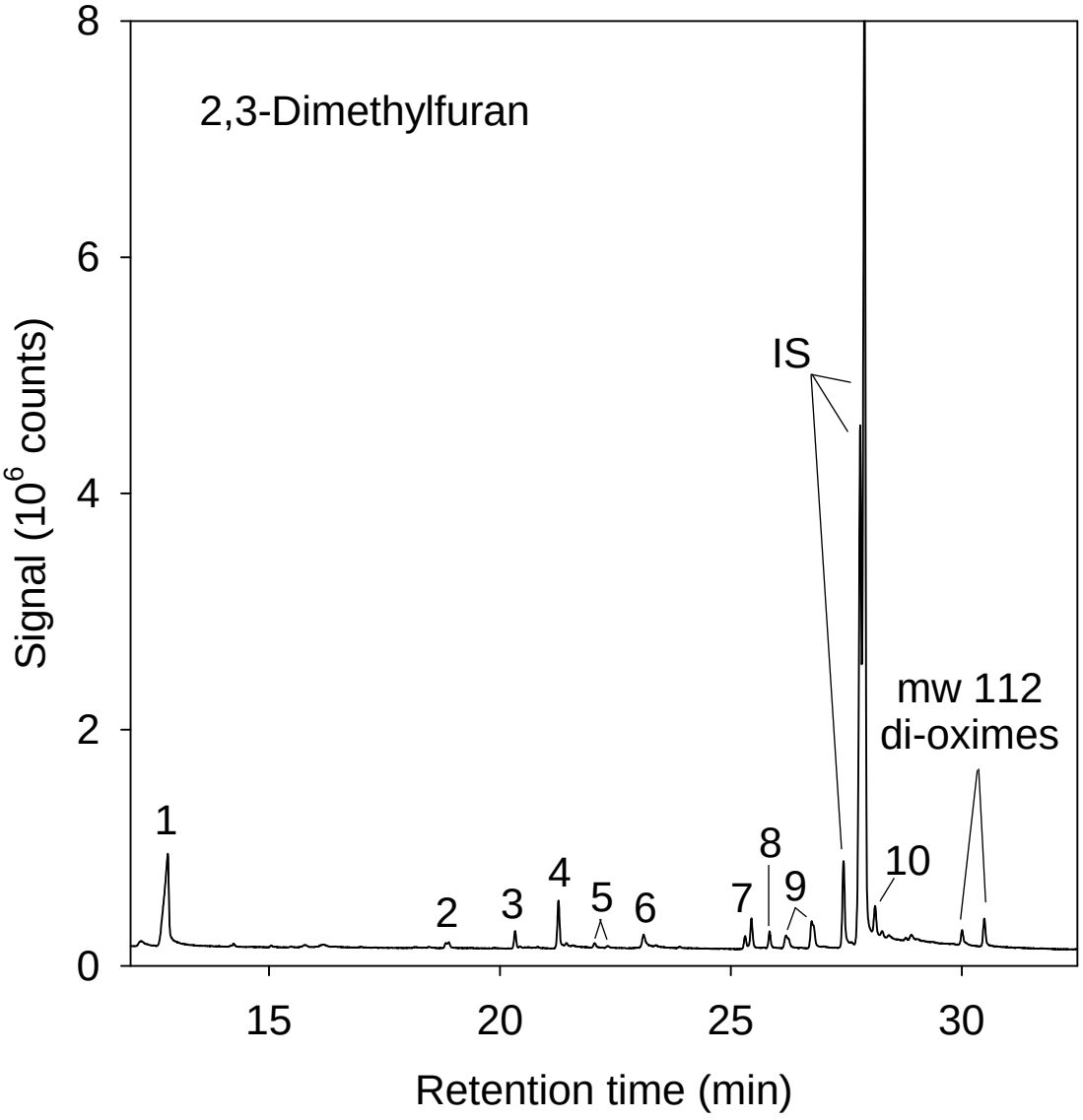

Figure S3. Positive chemical ionization GC-MS total ion chromatogram (TIC) of an extract of a PFBHA-coated denuder sample collected after 2 min irradiation of a CH_3ONO – NO – 2,3-dimethylfuran – 2,5-hexanedione (internal standard, IS) – air mixture, with 49% consumption of the initially present 2,3-dimethylfuran. IS = di-oximes of 2,5-hexanedione, the internal standard; peak #1, mono-oxime of mw 60 carbonyl, with fragment ions at m/z 129 and 111 present; peaks #2 and #3, from derivatizing agent; peak #4, unidentified mono-oxime; peaks #5, mono-oximes of mw 112 dicarbonyl (attributed to $CH_3C(O)C(CH_3)=CHCHO$); peak #6, mono-oxime of mw 114 carbonyl; peaks #7, di-oximes of glyoxal; peak #8, di-oxime of methylglyoxal (mw 72); peaks #9, di-oximes of $CH_3C(O)CH_2CHO$ (mw 86) formed from OH + 2,5-hexanedione, with a contribution to the earliest-eluting of these peaks from biacetyl; peak #10, di-oximes of mw 102 dicarbonyl, with fragment ion indicating loss of H_2O (and hence possibly $CH_3C(O)CH(OH)CHO$ formed as a second-generation product from $CH_3C(O)C(CH_3)=CHCHO$); and mw 112 di-oximes attributed to $CH_3C(O)C(CH_3)=CHCHO$.

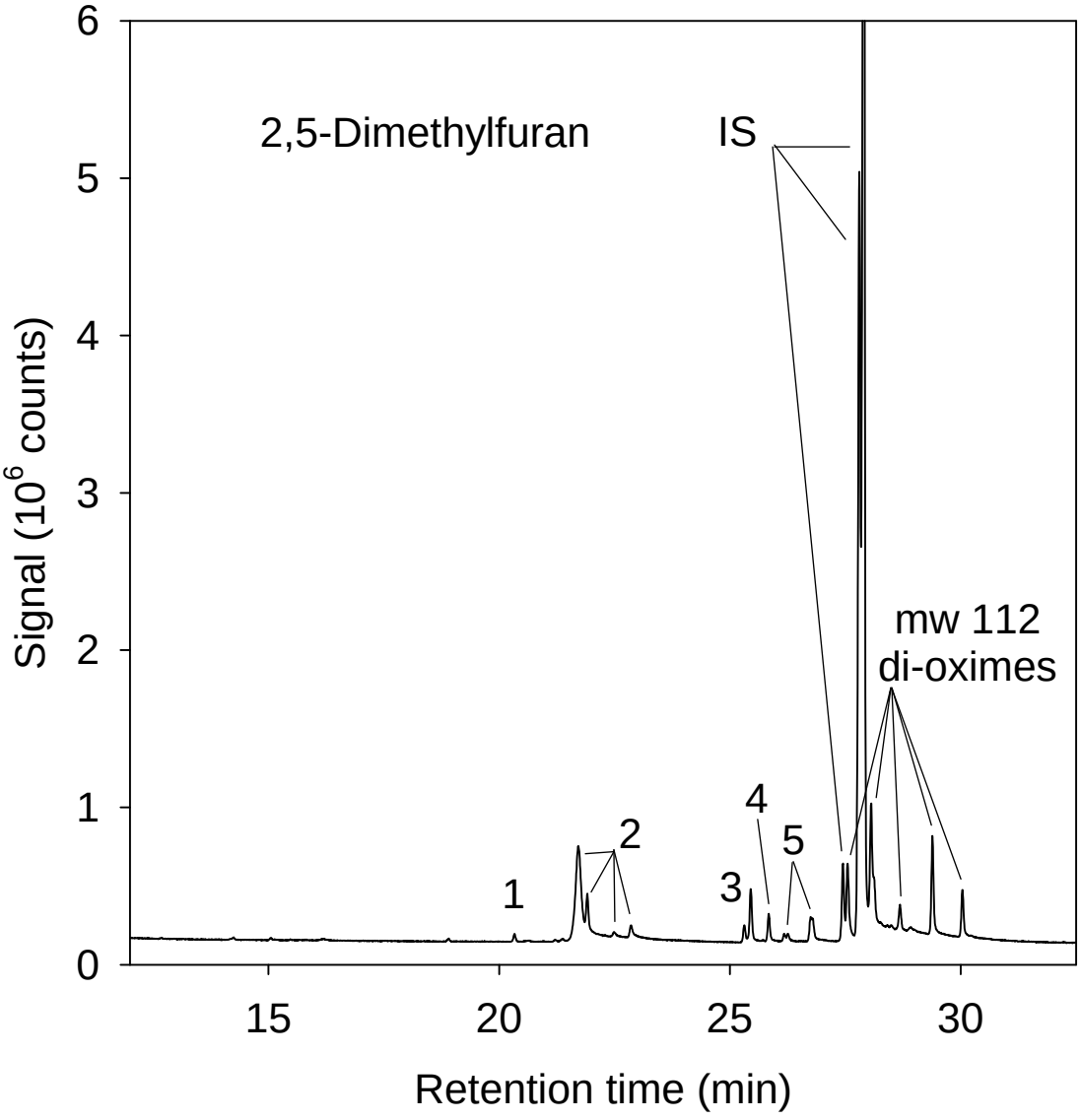

Figure S4. Positive chemical ionization GC-MS total ion chromatogram (TIC) of an extract of a PFBHA-coated denuder sample collected after 1.5 min irradiation of a CH_3ONO – NO – 2,5-dimethylfuran – 2,5-hexanedione (internal standard, IS) – air mixture, with 35% consumption of the initially present 2,5-dimethylfuran. IS = di-oximes of 2,5-hexanedione, the internal standard; peak #1, from derivatizing agent; peaks #2, mono-oximes of mw 114 carbonyl(s); peaks #3, di-oximes of glyoxal; peak #4, di-oxime of methylglyoxal (mw 72); peaks #5, di-oximes of $CH_3C(O)CH_2CHO$ (mw 86) formed from OH + 2,5-hexanedione; and mw 112 di-oximes of $CH_3C(O)CH=CHC(O)CH_3$.

Table S1. Experimental conditions and results for CH_3ONO – NO – furan – 2,5-hexanedione – air irradiations

furan	irradiation time (min)[b]	[furan], ppbV[a]		unsaturated 1,4-dicarbonyl (ppbV)[a,c]
		initial	reacted	
furan	8	1017	582	271, 266
	6	1033	500	257, 261, 255
	4	1029	386	218, 214
	8	1057	622	289, 299, 294, 298, 292
2-methylfuran	3	940.5	464.5	106
	2	895	336	74.3, 74.4
	3	797.5	401.5	86.9, 86.6
	2.5	1016.5	412.5	107, 107
3-methylfuran	3	900.5	506	135, 134
	2	889.5	400.5	115, 115
	2.5	1004	513	144, 142
	2	967	424	126, 129
2,3-dimethylfuran	3	906	583	37.7, 38.6
	2	916	449	30.3, 29.4
	1.5	933.5	354.5	25.4, 25.2
	2	935	459.5	34.0, 33.6
	4[d]	964	592	40.1, 40.9, 39.7
	3[e]	919	449.5	27.0, 26.6
	3[f]	948.5	474	28.9, 27.7
2,5-dimethylfuran	1.5	945	330.5	81.3, 81.1

[a]1 ppbV = 2.40×10^{10} molecule cm^{-3} for the temperature and pressure conditions employed (296 ± 2 K and ~735 Torr pressure).

[b]At a light intensity corresponding to an NO_2 photolysis rate of 0.14 min^{-1}. Unless noted otherwise, PFBHA-coated denuder samples were collected immediately after the irradiation,

with the denuder sampling directly from the chamber and with the denuder inlet protruding into the chamber. 2,5-Hexanedione (225-244 ppbV) was included in the reactant mixture prior to irradiation. The initial CH_3ONO and NO concentrations were ~5 ppmV each.

[c]Measured concentrations of unsaturated 1,4-dicarbonyl [HC(O)CH=CHCHO from furan, $CH_3C(O)CH=CHCHO$ from 2-methylfuran, $HC(O)C(CH_3)=CHCHO$ from 3-methylfuran, $CH_3C(O)C(CH_3)=CHCHO$ from 2,3-dimethylfuran, and $CH_3C(O)CH=CHC(O)CH_3$ from 2,5-dimethylfuran]. In each experiment, the dicarbonyl concentration was determined from the GC-FID peak areas of the di-oxime peaks of 2,5-hexanedione (the internal standard) and of the di- and (if present) mono-oxime peaks of the unsaturated 1,4-dicarbonyl, and the measured concentration of 2,5-hexanedione (from GC-FID analyses of samples collected onto Tenax solid adsorbent; see text), taking into account small differences in the GC-FID response factors for the dicarbonyl di-oximes.[1,2] The entries for a given experiment are from replicate analyses of the extract.

[d]Preliminary experiment carried out with PFBHA-coated denuder samples being collected 156 min after the irradiation period, with the denuder sampling downstream of a cascade impactor. 2,5-Hexanedione (374.5 ppbV) was added after the irradiation.

[e]Preliminary experiment carried out with PFBHA-coated denuder samples being collected 45 min after the irradiation period, with the denuder sampling downstream of a cascade impactor. 2,5-Hexanedione (124 ppbV) was added after the irradiation.

[f]Preliminary experiment carried out with PFBHA-coated denuder samples being collected 1 min after the irradiation period, with the denuder sampling downstream of a cascade impactor. 2,5-Hexanedione (96 ppbV) was included in the reactant mixture prior to irradiation.

Behavior of Unsaturated 1,4-Dicarbonyls during OH + Furan Reactions

For the reaction sequence,

OH + furan $\rightarrow$ α dicarbonyl + other products	(k_{furan})
OH + dicarbonyl $\rightarrow$ products	(k_{OH})
dicarbonyl + $h\nu$ $\rightarrow$ loss of dicarbonyl	(k_{phot})
dicarbonyl $\rightarrow$ wall loss of dicarbonyl	(k_w)

the concentration of the dicarbonyl at time t is given by,

$$[\text{dicarbonyl}]_t = A\,(e^{-x} - e^{-Bx}) \qquad \text{(I)}$$

where $A = \alpha[\text{furan}]_{initial}\{k_{furan}[OH]/(k_{OH}[OH] + k_{phot} + k_w)]\}$, α is the formation yield of dicarbonyl from reaction (1) $B = (k_{OH}[OH] + k_{phot} + k_w)/k_{furan}[OH]$, and x = extent of reaction = $\ln([\text{furan}]_{to}/[\text{furan}]_t)$.[3,4] Hence a fit of Equation (I) to the experimental data leads to values of A and B,[3,4] with the values of B (referred to here and in the manuscript as k_2/k_1) being of particular interest in this study.

Two sets of relevant data were obtained (Table S2); one set from the denuder analyses, with one data point per experiment at a given extent of reaction and with the duration of the experiments being ~1.5 hr, and the second set from continuous irradiations of CH_3ONO – NO – furan – air mixtures with analysis of the unsaturated 1,4-dicarbonyl every ~3 min by direct air sampling atmospheric pressure ionization mass spectrometry (API-MS).[4] In this second set of experiments, the furan (or alkylfuran) concentrations were measured by GC-FID before and after

the irradiations, which were carried out for 21-66 min at a light intensity corresponding to an NO_2 photolysis rate of ~0.035 min^{-1} (a factor of 4 lower than used for the experiments with sample collection onto annular denuders).

Figures S5-S8 show plots of Equation (I) for the experiments with GC analyses of PFBHA-coated denuder samples (i.e., the data presented in Table S1, with each data point in Figures S5-S8 being an average of the replicate unsaturated 1,4-dicarbonyl concentrations for that experiment), together with predictions from Equation (I) with differing values of k_2/k_1 (see also text in the manuscript and the captions to the individual figures). In these denuder experiments, conducted with identical initial CH_3ONO and NO concentrations, for a given furan the OH radical concentrations averaged over the irradiation period were independent of the irradiation time, with ≤13% change in the OH radical concentration for a factor of 2 change in the irradiation time (see the denuder samples in Table S2). Hence the OH radical concentrations could be taken to be constant for the experiments with a given furan in the same Teflon chamber, and for a given furan the relative contributions of photolysis and OH radical reaction were essentially constant for that series of experiments. The data for OH + 2,3-dimethylfuran shown in Figure S8, for two series of experiments in different Teflon chambers with differing OH radical concentrations, are consistent with our assumption that photolysis of 3-methyl-4-oxo-2-pentenal by black lamps was of no importance.

The data from the second set of experiments (those with continuous irradiations and in situ API-MS analyses) are summarized in Table S2 and representative plots of Equation (I) are shown in Figures S9 and S10. In these experiments, with pre- and post-reaction GC-FID analyses of the furan and API-MS analyses of the unsaturated 1,4-dicarbonyl, the OH radical concentrations during the 21-66 min irradiation period were assumed to be constant in order to

calculate the extents of reaction, $\ln([furan]_{to}/[furan]_t)$. While the OH radical concentrations would very likely decrease during the irradiation periods, the effect should have been small because of the low light intensities employed. If the OH radical concentration in an experiment decreased with irradiation time, then the assumption of a constant OH radical concentration would mean that the derived values of k_2/k_1 would be upper limits (see Figure S11).

The data from the two sets of experiments are reasonably consistent (Table S2), with values of k_2/k_1 of ~1.0 for HC(O)CH=CHCHO formation from OH + furan, 0.6-0.9 for formation of $CH_3C(O)CH=CHCHO$ from OH + 2-methylfuran, 0.6-0.8 for formation of $HC(O)C(CH_3)=CHCHO$ from OH + 3-methylfuran, and ~0.5 for formation of $CH_3C(O)C(CH_3)=CHCHO$ from OH + 2,3-dimethylfuran.

Table S2. Experimental conditions and results from analyses of the time-concentration behavior of unsaturated 1,4-dicarbonyls during OH radical-initiated reactions of furans

furan	CH_3ONO (ppmV)	NO (ppmV)	irradiation time (min)[a]	$10^{-7} \times [OH]_{av}$ (molecule cm^{-3})[b]	k_2/k_1	analysis method
furan	2	2	45	1.52	0.8 ± 0.1[c]	API-MS
furan	1	2	66	0.73	1.2 ± 0.1	API-MS
furan	2	1	30	2.81	0.9 ± 0.1	API-MS
furan	5	5	4-8	4.36-4.86	1.03[d]	denuder
2-methylfuran	2	2	33	1.70	0.5 ± 0.1[e]	API-MS
2-methylfuran	1	1	36	1.67	0.6 ± 0.1	API-MS
2-methylfuran	1	2	39	0.93	0.9 ± 0.1	API-MS
2-methylfuran	2	1	21	3.19	0.3 ± 0.1	API-MS
2-methylfuran	5	5	2-3	4.74-5.36	0.90[f]	denuder
3-methylfuran	2	2	27	1.81	0.65 ± 0.1	API-MS
3-methylfuran	1	2	39	0.94	0.55 ± 0.1	API-MS
3-methylfuran	5	5	2-3	5.46-5.71	0.79[g]	denuder
2,3-dimethylfuran	2	2	24	1.60	0.55 ± 0.1	API-MS
2,3-dimethylfuran	1	2	36	0.88	0. 45 ± 0.1	API-MS
2,3-dimethylfuran	5	5	1.5-4	2.96-4.47[h]	0.48[i]	denuder

[a]At light intensities corresponding to NO_2 photolysis rates of 0.14 min^{-1} for experiments with GC-FID analysis of annular denuder samples and ~0.035 min^{-1} for experiments with API-MS analysis.

[b]Calculated from pre- and post-reaction GC-FID analyses of the furans.

[c]See Figure S9.

[d]See Figure S5; four experiments were conducted.

[e]See Figure S10.

[f]See Figure S6; four experiments were conducted.

[g]See Figure S7; four experiments were conducted.

[h]For data denoted by open symbols (○) in Figure S8, the four irradiations were for 1.5-3 min, with calculated OH radical concentrations of (4.21-4.54) × 10^7 molecule cm^{-3}. For the three preliminary experiments (filled symbols (●) in Figure S8), irradiations were for 3-4 min, with calculated OH radical concentrations of (2.96-3.15) × 10^7 molecule cm^{-3}.

[i]See Figure S8.

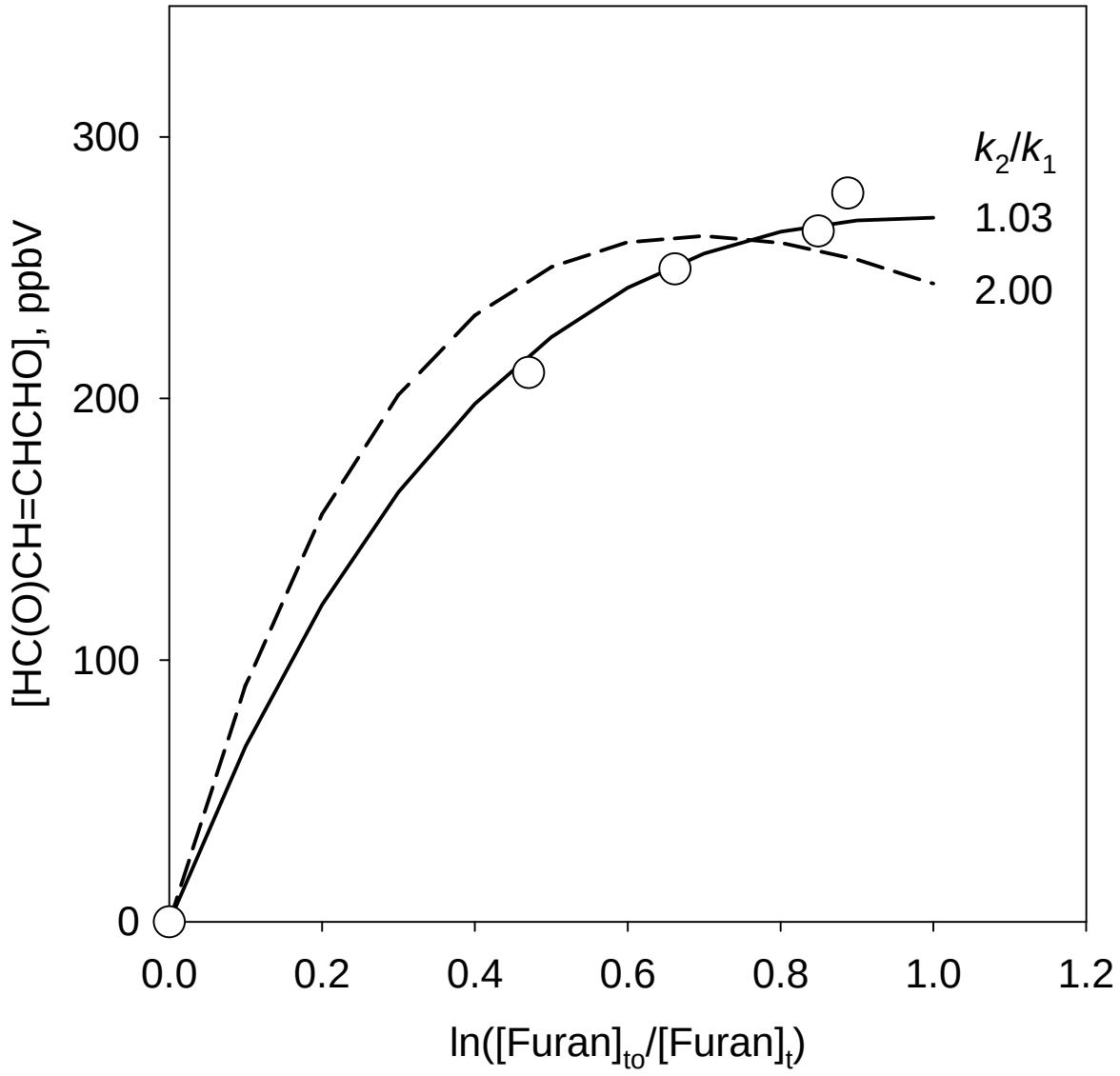

Figure S5. Plot of measured concentrations of HC(O)CH=CHCHO as a function of the extent of reaction, defined as $\ln([\text{furan}]_{to}/[\text{furan}]_t)$, in the OH + furan reactions. Each data point is the average measured concentration from a single experiment (see Table S1). The lines are calculated from the expression [HC(O)CH=CHCHO] = $A\{\exp(-k_1t) - \exp(-k_2t)\}$, where k_1 is the rate of reaction of the furan, k_2 is the rate of reaction of HC(O)CH=CHCHO (by reaction with OH radicals, photolysis and any other loss processes), and A was used as an adjustable constant to match the experimental data in the Y-axis. Note that $\ln([\text{furan}]_{to}/[\text{furan}]_t) = k_1(t - t_o)$ since the OH radical concentration was essentially constant and equal for all four experiments.

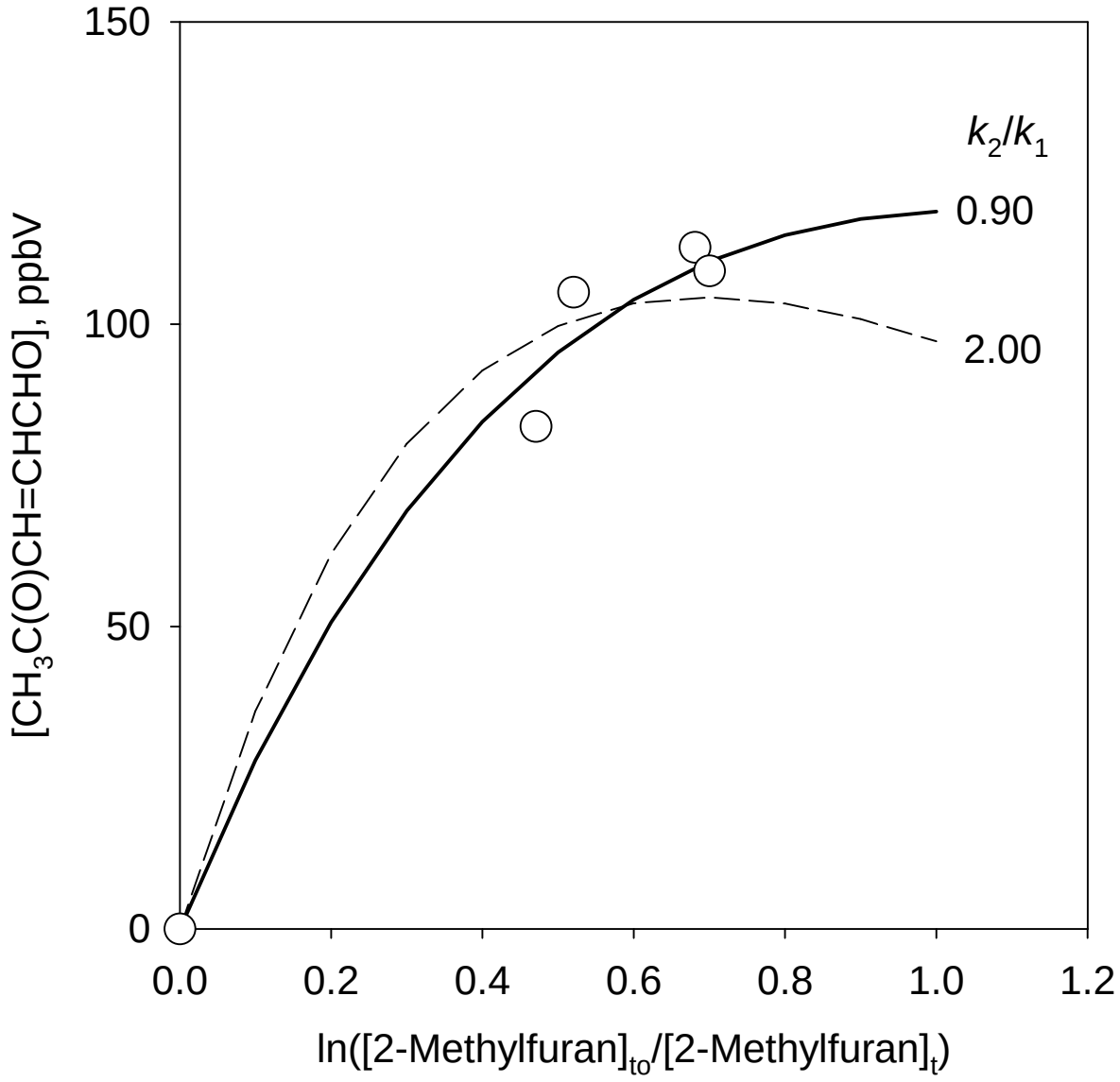

Figure S6. Plot of measured concentrations of $CH_3C(O)CH=CHCHO$ as a function of the extent of reaction, defined as $\ln([2\text{-methylfuran}]_{to}/[2\text{-methylfuran}]_t)$, in the OH + 2-methylfuran reactions. Each data point is the average measured concentration from a single experiment (see Table S1). The lines are calculated from the expression $[CH_3C(O)CH=CHCHO] = A\{\exp(-k_1t) - \exp(-k_2t)\}$, where k_1 is the rate of reaction of the 2-methylfuran, k_2 is the rate of reaction of $CH_3C(O)CH=CHCHO$ (by reaction with OH radicals, photolysis and any other loss processes), and A was used as an adjustable constant to match the experimental data in the Y-axis. Note that $\ln([2\text{-methylfuran}]_{to}/[2\text{-methylfuran}]_t) = k_1(t - t_o)$ since the OH radical concentration was essentially constant and equal for all four experiments.

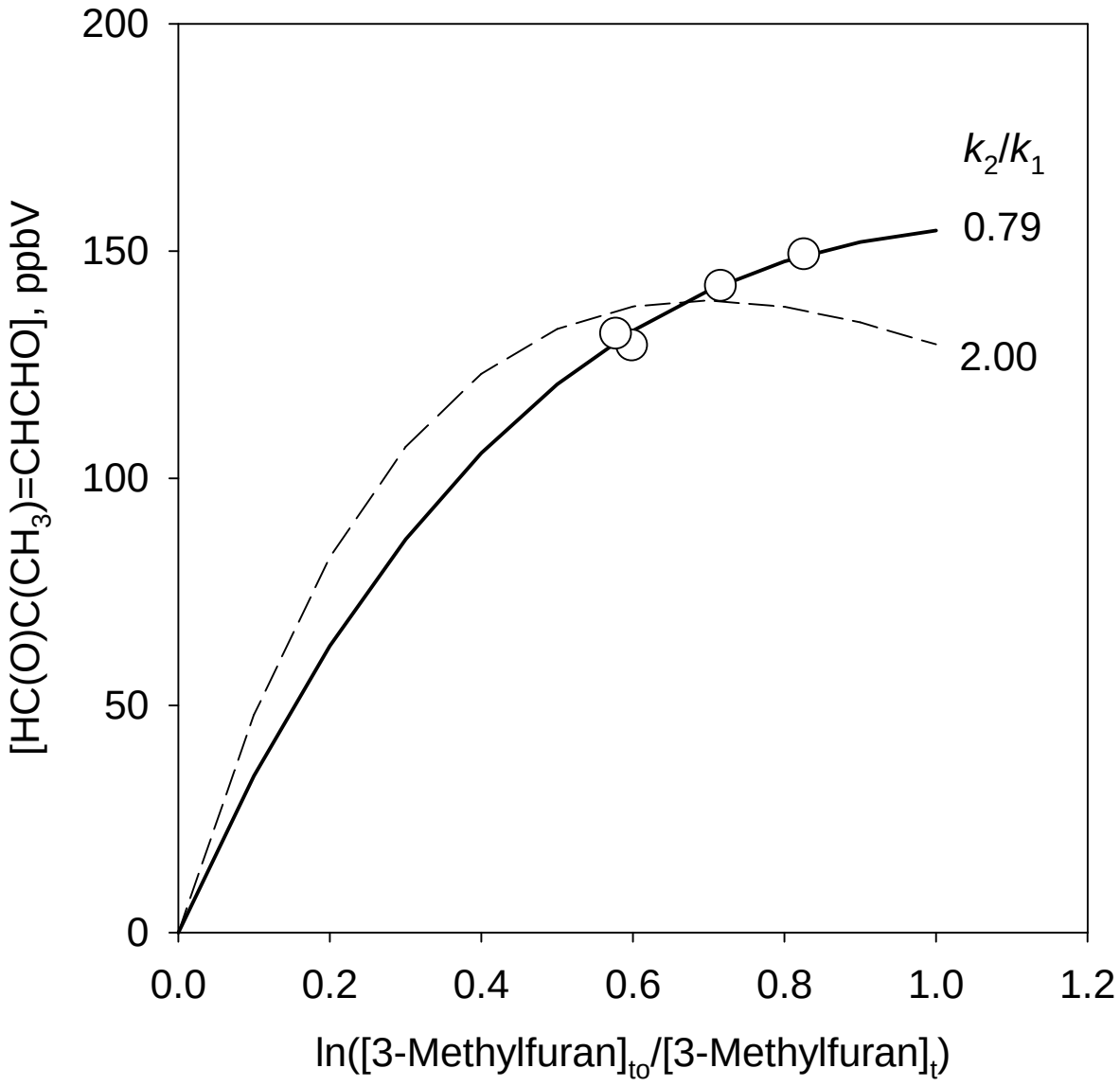

Figure S7. Plot of measured concentrations of $HC(O)C(CH_3)=CHCHO$ as a function of the extent of reaction, defined as $\ln([3\text{-methylfuran}]_{to}/[3\text{-methylfuran}]_t)$, in the OH + 3-methylfuran reactions. Each data point is the average measured concentration from a single experiment (see Table S1). The lines are calculated from the expression $[HC(O)C(CH_3)=CHCHO] = A\{\exp(-k_1t) - \exp(-k_2t)\}$, where k_1 is the rate of reaction of the 3-methylfuran, k_2 is the rate of reaction of $HC(O)C(CH_3)=CHCHO$ (by reaction with OH radicals, photolysis and any other loss processes), and A was used as an adjustable constant to match the experimental data in the Y-axis. Note that $\ln([3\text{-methylfuran}]_{to}/[3\text{-methylfuran}]_t) = k_1(t - t_o)$ since the OH radical concentration was essentially constant and equal for all four experiments.

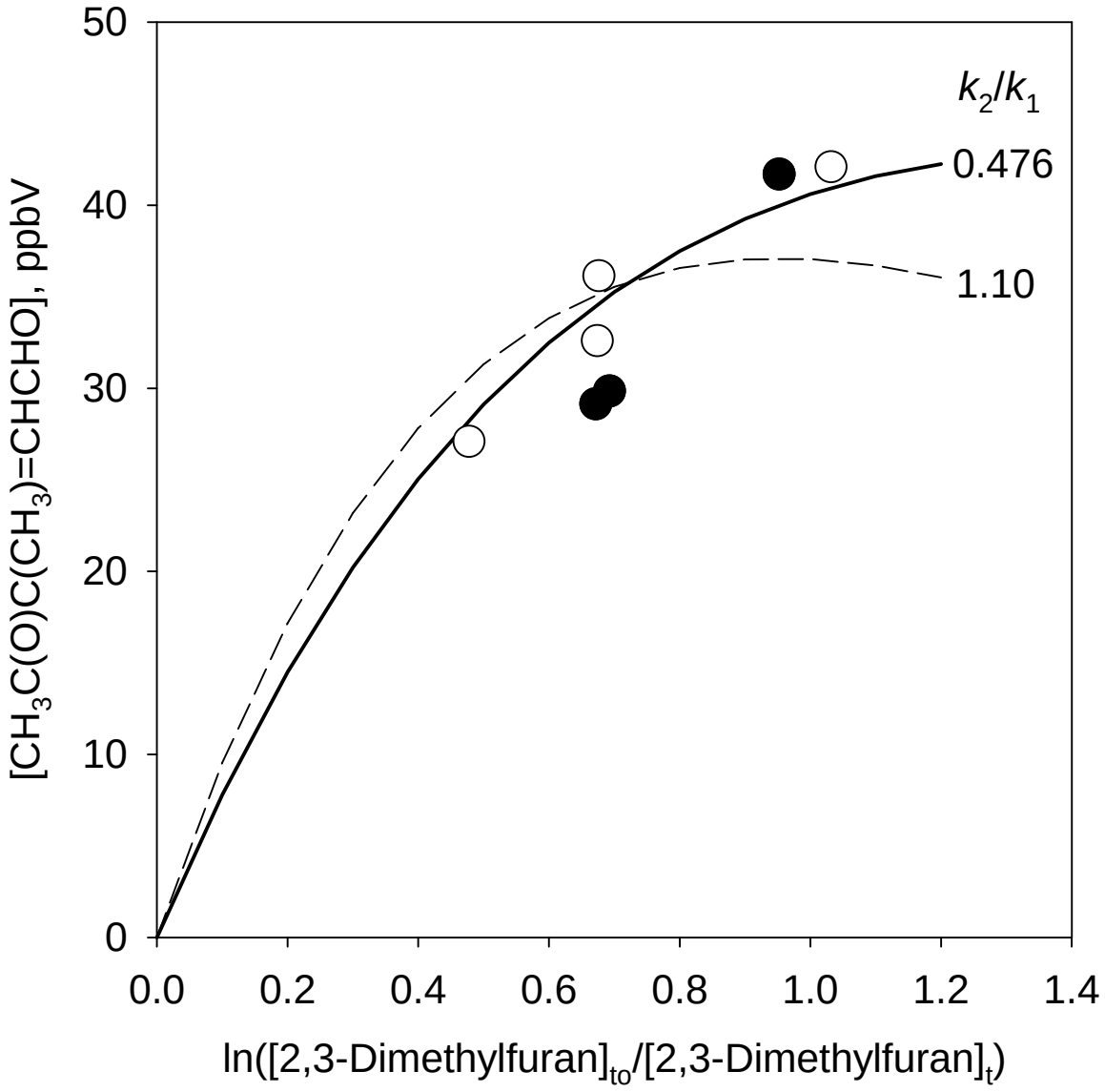

Figure S8. Plot of measured concentrations of $CH_3C(O)C(CH_3)=CHCHO$ as a function of the extent of reaction, defined as $\ln([2,3\text{-dimethylfuran}]_{to}/[2,3\text{-dimethylfuran}]_t)$, in the OH + 2,3-dimethylfuran reactions. Each data point is the average measured concentration from a single experiment (see Table S1). The lines are calculated from the expression $[CH_3C(O)C(CH_3)=CHCHO] = A\{\exp(-k_1t) - \exp(-k_2t)\}$, where k_1 is the rate of reaction of the 2,3-dimethylfuran, k_2 is the rate of reaction of $CH_3C(O)C(CH_3)=CHCHO$ (by reaction with OH radicals, photolysis and any other loss processes), and A was used as an adjustable constant to match the experimental data in the Y-axis. Note that $\ln([2,3\text{-dimethylfuran}]_{to}/[2,3\text{-dimethylfuran}]_t) = k_1(t - t_o)$ since the OH radical concentration was essentially constant and equal for the experiments with the same symbol. ○, experiments with 2,5-hexanedione initially present in the reactant mixtures and with sampling immediately after the irradiation period; ●, preliminary experiments (see Table S1 for conditions and Table S2 for the OH radical concentrations during the experiments).

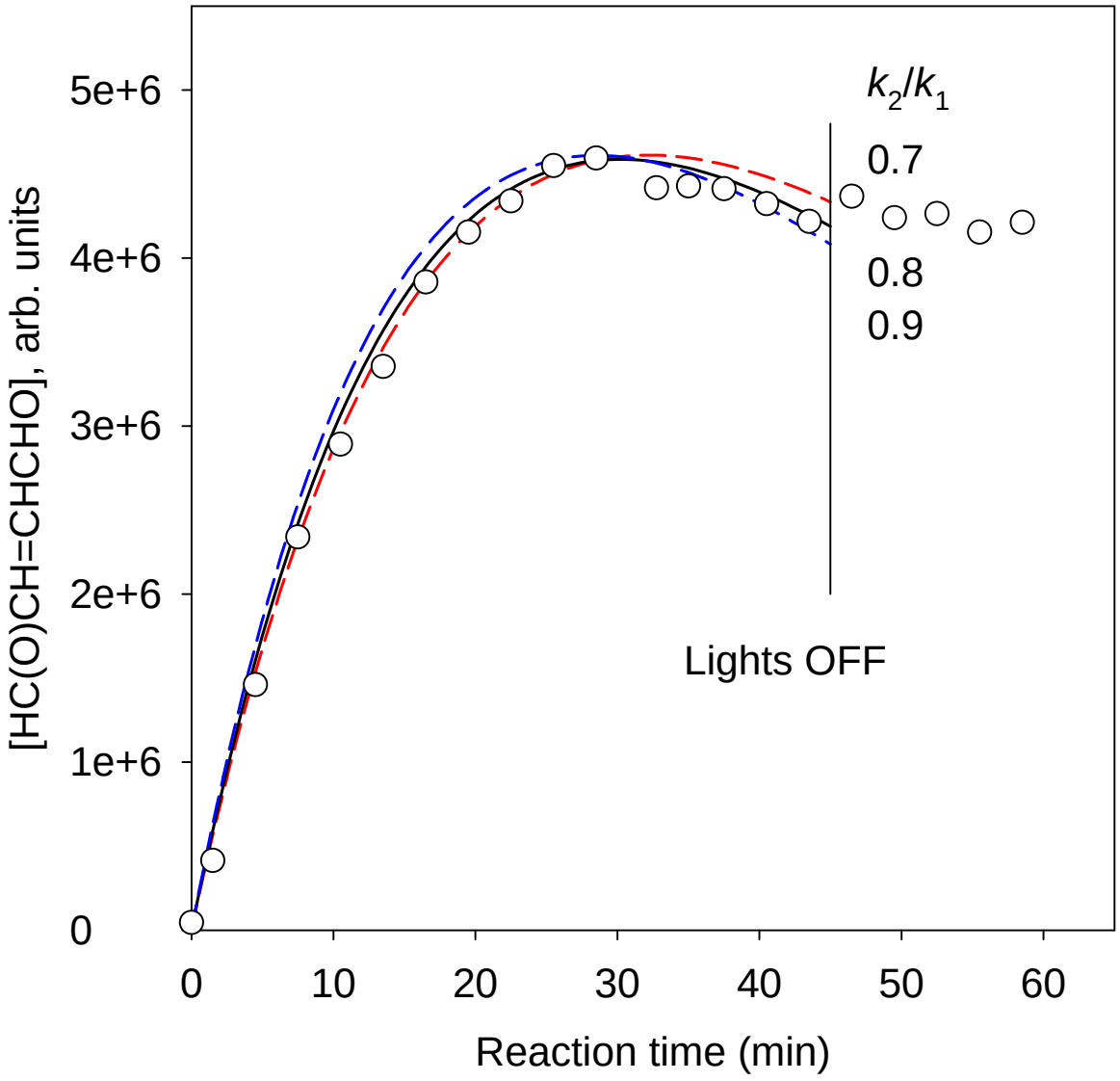

Figure S9. Plot of the API-MS signal attributed to ions of HC(O)CH=CHCHO as a function of the reaction time in an OH + furan reaction (see Table S2 for the experimental conditions). The lights were turned on at 0 min and off at 45 min, and data obtained after the lights were turned off are also shown. The lines are calculated from the expression [HC(O)CH=CHCHO] = $A\{\exp(-k_1 t) - \exp(-k_2 t)\}$, where k_1 is the rate of reaction of the furan, k_2 is the rate of reaction of HC(O)CH=CHCHO (by reaction with OH radicals, photolysis and any other loss processes), and A was used as an adjustable constant to match the experimental data in the Y-axis. A constant OH radical concentration was assumed, with $\ln([\text{furan}]_{to}/[\text{furan}]_t) = k_1(t - t_o)$.

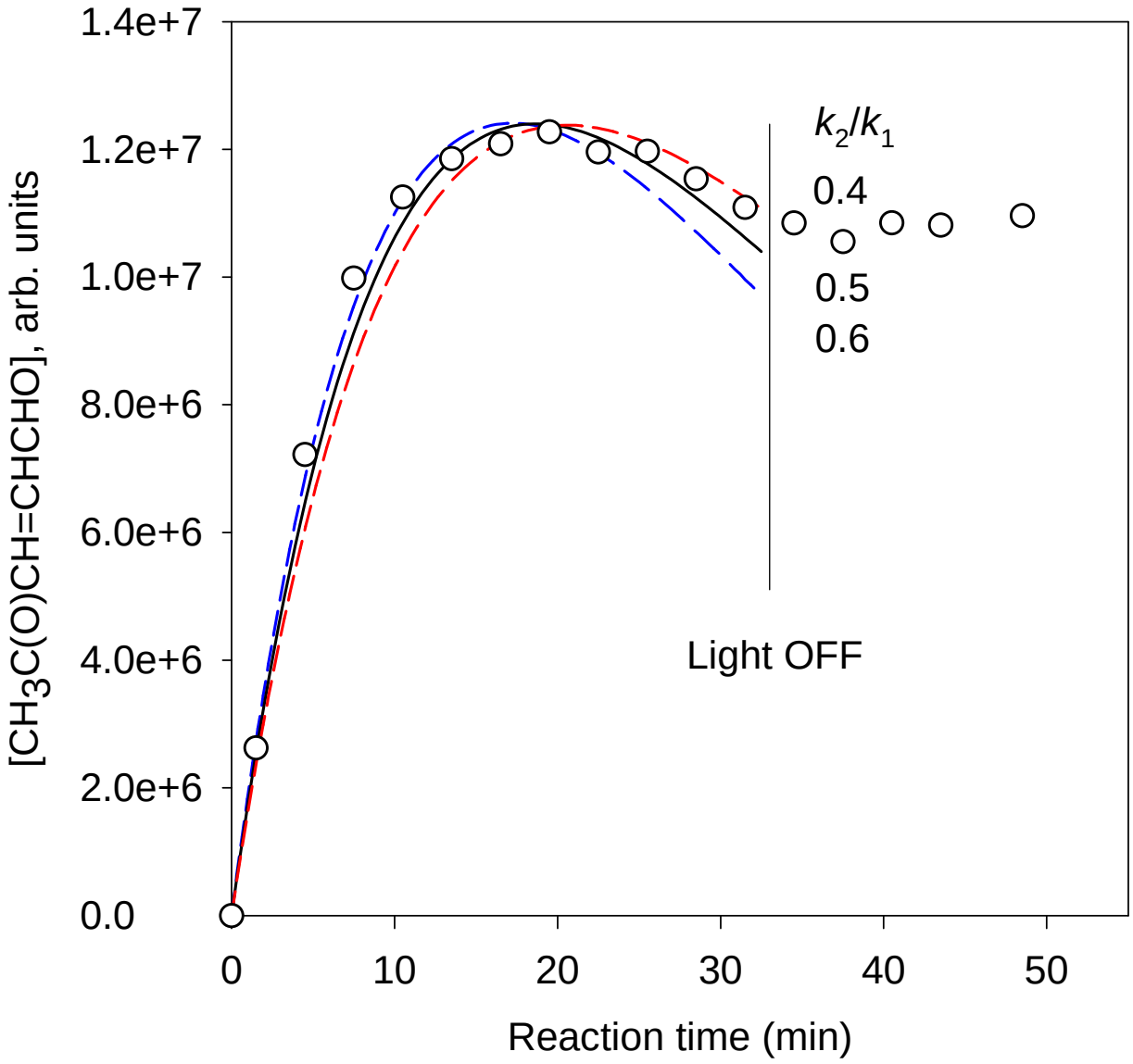

Figure S10. Plot of the API-MS signal attributed to ions of $CH_3C(O)CH=CHCHO$ as a function of the reaction time in an OH + 2-methylfuran reaction (see Table S2 for the experimental conditions). The lights were turned on at 0 min and off at 33 min, and data obtained after the lights were turned off are also shown. The lines are calculated from the expression $[CH_3C(O)CH=CHCHO] = A\{\exp(-k_1t) - \exp(-k_2t)\}$, where k_1 is the rate of reaction of the 2-methylfuran, k_2 is the rate of reaction of $CH_3C(O)CH=CHCHO$ (by reaction with OH radicals, photolysis and any other loss processes), and A was used as an adjustable constant to match the experimental data in the Y-axis. A constant OH radical concentration was assumed, with $\ln([2\text{-methylfuran}]_{to}/[2\text{-methylfuran}]_t) = k_1(t - t_o)$.

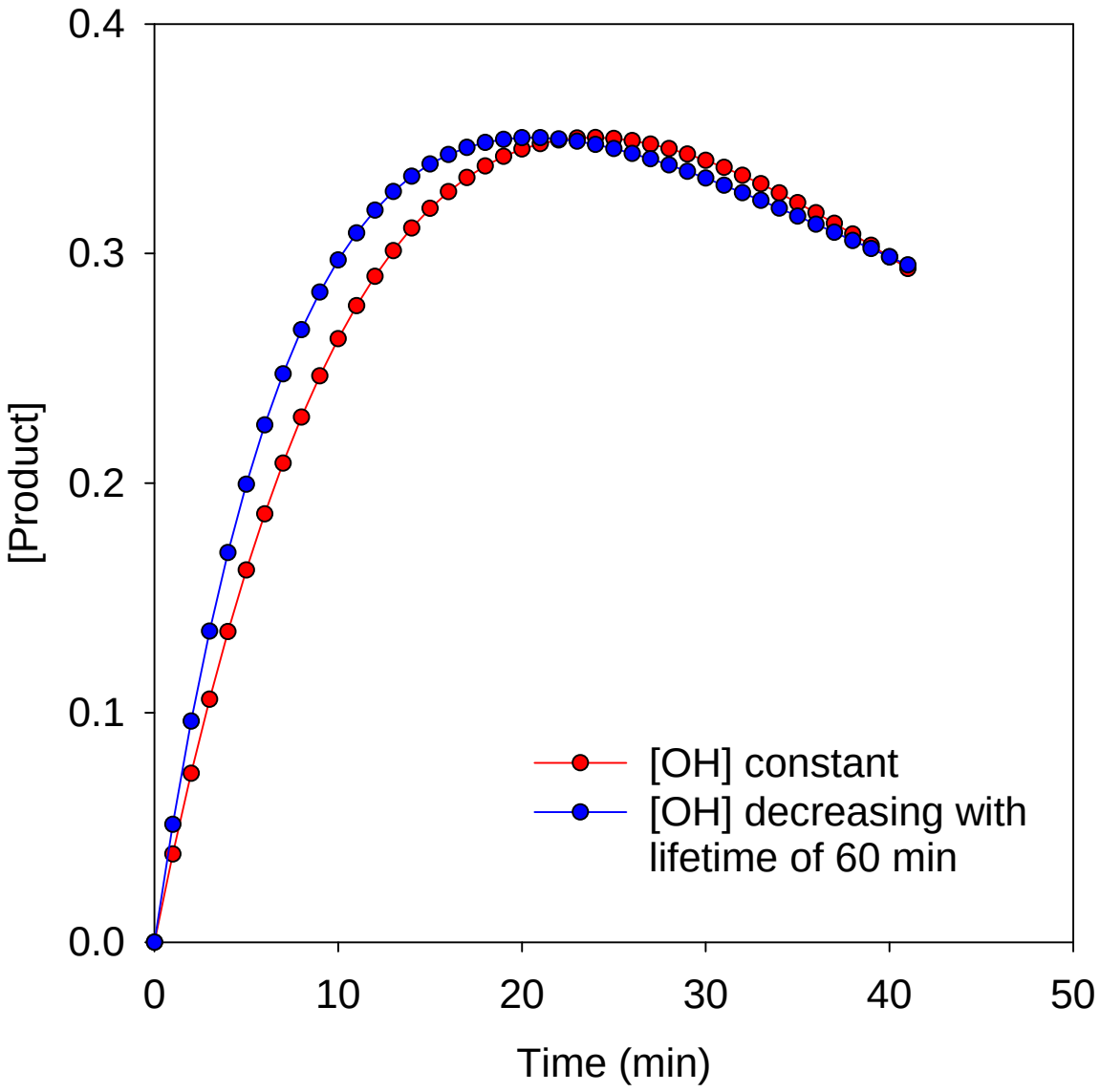

Figure S11. Plots of Equation (I), with (red) a constant OH radical concentration for 40 min, and (blue) an OH radical concentration which decayed exponentially with a lifetime of 60 min (approximately corresponding to that expected for the light intensity employed in the experiments with in situ API-MS detection of the unsaturated 1,4-dicarbonyls). The integrated OH radical concentration at t = 40 min was identical in both calculations. The maximum [Product] occurs earlier in the simulation with decreasing OH radical concentration, which would be interpreted as a higher value of k_2/k_1 if an constant OH radical concentration was assumed to derive the extents of reaction, x, in Equation (I).

Formation of unsaturated 1,4-dicarbonyls from OH + aromatic hydrocarbons

Unsaturated 1,4-dicarbonyls and 1,2-dicarbonyls are also formed from the OH radical-initiated reactions of monocyclic aromatic hydrocarbons.[2,5-10] Glyoxal, methylglyoxal and 2,3-butanedione formation yields from the toluene, *o*-, *m*- and *p*-xylene, and 1,2,3-, 1,2,4- and 1,3,5-trimethylbenzene reactions have been obtained at low NO_2 concentrations.[2,7,11] The 3-hexene-2,5-dione formation yields of Bethel et al.[7] from the OH + *p*-xylene and OH + 1,2,4-trimethylbenzene reactions are identical within the experimental uncertainties with the co-product glyoxal[2,12] and methylglyoxal[2] formation yields, respectively. The 3-hexene-2,5-dione formation yields can then be used to place the unsaturated 1,4-dicarbonyl relative yield data of Arey et al.[9] onto an absolute basis (assuming that all of the unsaturated 1,4-dicarbonyls have the same collection and derivatization efficiency and that the GC-MS total ion chromatogram signal responses are the same). The resulting comparison of the 1,2-dicarbonyl[2,7,11] and unsaturated 1,4-dicarbonyl[9] formation yields are shown in Figure S12 and Table S3. While the formation yields of 1,4-butenedial are similar to those of its presumed co-products (Table S4), the formation yields of 4-oxo-2-pentenal, 2-methyl-1,4-butenedial and 3-methyl-4-oxo-2-pentenal are significantly lower than those of their assumed co-products (Table S4).

Table S3. Molar formation yields (%) of 1,2-dicarbonyls and of their unsaturated 1,4-dicarbonyl presumed co-products at atmospheric pressure of air and low NO_2 concentrations

aromatic	1,2-dicarbonyl[a]	presumed co-product[b]
toluene	$(CHO)_2$, 26.0 ± 2.2	$CH_3C(O)CH=CHCHO$, 7.7 $HC(O)C(CH_3)=CHCHO$, 1.2
	$CH_3C(O)CHO$, 21.5 ± 2.9	$HC(O)CH=CHCHO$, 24.1
o-xylene	$(CHO)_2$, 12.7 ± 1.9	$CH_3C(O)C(CH_3)=CHCHO$, 0.6 $HC(O)C(CH_3)=C(CH_3)CHO$, not observed
	$CH_3C(O)CHO$, 33.1 ± 6.1	$CH_3C(O)CH=CHCHO$, 14.4
	$CH_3C(O)C(O)CH_3$, 18.5[c]	$HC(O)CH=CHCHO$, 16.3
m-xylene	$(CHO)_2$, 11.4 ± 0.7	$CH_3C(O)CH=C(CH_3)CHO$, 1.6
	$CH_3C(O)CHO$, 51.5 ± 8.5	$CH_3C(O)CH=CHCHO$, 25.4 $HC(O)C(CH_3)=CHCHO$, 11.5
p-xylene	$(CHO)_2$, 38.9 ± 4.7	$CH_3C(O)CH=CHC(O)CH_3$, 40.5 (32.3[d])
	$CH_3C(O)CHO$, 18.7 ± 2.2	$HC(O)C(CH_3)=CHCHO$, 4.4
1,2,3-TMB	$(CHO)_2$, 4.7 ± 2.4	$CH_3C(O)C(CH_3)=C(CH_3)CHO$, 0.1
	$CH_3C(O)CHO$, 15.1 ± 3.3	$CH_3C(O)C(CH_3)=CHCHO$, 3.2
	$CH_3C(O)C(O)CH_3$, 52.0[d]	$CH_3C(O)CH=CHCHO$, 16
1,2,4-TMB	$(CHO)_2$, 8.7 ± 1.6	$CH_3C(O)C(CH_3)=CHC(O)CH_3$, 3.0
	$CH_3C(O)CHO$, 27.2 ± 8.1	$CH_3C(O)C(CH_3)=CHCHO$, 0.2 $CH_3C(O)CH=CH(CH_3)CHO$, 0.4 $CH_3C(O)CH=CHC(O)CH_3$, 25.6 (30.9[d]) $HC(O)C(CH_3)=C(CH_3CHO$, not observed
	$CH_3C(O)C(O)CH_3$, 10.2	$HC(O)C(CH_3)=CHCHO$, 2.4
1,3,5-TMB	$CH_3C(O)CHO$, 58.1 ± 5.3	$CH_3C(O)CH=C(CH_3)CHO$, 7.2

[a]From Nishino et al.,[2] unless noted otherwise, at low NO_2 concentration.
[b]From Arey et al.,[9] using the formation yields of 3-hexene-2,5-dione from the *p*-xylene and 1,2,4-trimethylbenzene reactions measured by Bethel et al.[7] to place the relative yield data of Arey et al.[9] on an absolute basis.
[c]From Atkinson and Aschmann.[11]
[d]From Bethel et al.[7]

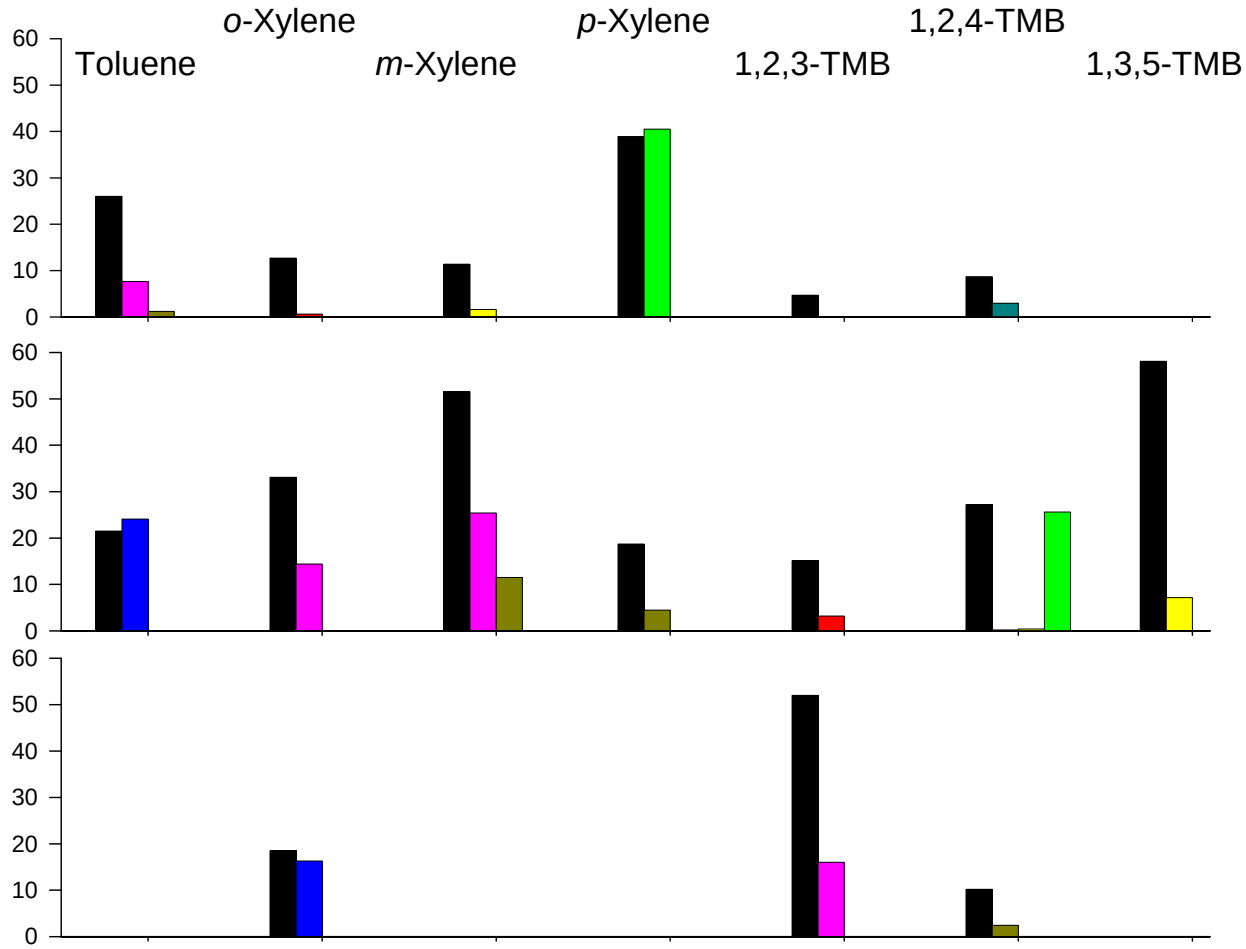

Figure S12. Top panel: glyoxal and co-product unsaturated 1,4-dicarbonyl formation yields from the aromatics. Middle panel: methylglyoxal and co-product unsaturated 1,4-dicarbonyl formation yields. Bottom panel: 2,3-butanedione and co-product unsaturated 1,4-dicarbonyl formation yields. The data are from Table S3. Black bars refer to the 1,2-dicarbonyls, blue to HC(O)CH=CHCHO, pink to $CH_3C(O)CH=CHCHO$, tan to $HC(O)C(CH_3)=CHCHO$, red to $CH_3C(O)C(CH_3)=CHCHO$, bright yellow to $CH_3C(O)CH=C(CH_3)CHO$, green to $CH_3C(O)CH=CHC(O)CH_3$, and turquoise to $CH_3C(O)C(CH_3)=CHC(O)CH_3$.

Table S4. Ratios of (molar yield of unsaturated 1,4-dicarbonyl)/(molar yield of 1,2-dicarbonyl co-product) calculated using the data presented in Table S3 for OH + methyl-substituted benzenes

unsaturated 1,4-dicarbonyl	from reaction of OH radicals with					
	toluene	*o*-xylene	*m*-xylene	*p*-xylene	123-TMB	124-TMB
HC(O)CH=CHCHO	1.12	0.88				
$CH_3C(O)CH=CHCHO$	≥0.31[a]	0.44	≥0.64[a]		0.31	
$HC(O)C(CH_3)=CHCHO$	≥0.07[a]		≥0.44[a]	0.24		0.24
$CH_3C(O)C(CH_3)=CHCHO$		≥0.05[a]			0.21	

[a]Taking into account the measured formation yield of the other unsaturated 1,4-dicarbonyl (see Table S3), which may be a lower limit. For example, for OH + *m*-xylene, the co-products to methylglyoxal (51.5% measured yield) are $CH_3C(O)CH=CHCHO$ (25.4% measured yield) and $HC(O)C(CH_3)=CHCHO$ (11.5% measured yield). The ratio ($CH_3C(O)CH=CHCHO$ yield)/(methylglyoxal yield) = 25.4/(51.5-11.5) = 0.64. Since the measured $HC(O)C(CH_3)=CHCHO$ formation yield may be a lower limit, the ratio ($CH_3C(O)CH=CHCHO$ yield)/(methylglyoxal yield) ≥0.64.

References

1. Scanlon, J. T.; Willis, D. E. Calculation of Flame Ionization Detector Relative Response Factors using the Effective Carbon Number Concept. *J. Chromat. Sci*. **1985**, *23*, 333-340.
2. Nishino, N.; Arey, J.; Atkinson, R. Formation Yields of Glyoxal and Methylglyoxal from the Gas-Phase OH Radical-Initiated Reactions of Toluene, Xylenes, and Trimethylbenzenes as a Function of NO_2 Concentration. *J. Phys. Chem. A* **2010**, *114*, 10140-10147.
3. Baker, J.; Arey, J.; Atkinson, R. Rate Constants for the Gas-Phase Reactions of OH Radicals with a Series of Hydroxyaldehydes at 296 ± 2 K. *J. Phys. Chem. A* **2004**, *108*, 7032-7037.
4. Nishino, N.; Arey, J.; Atkinson, R. Formation and Reactions of 2-Formylcinnamaldehyde in the OH Radical-Initiated Reaction of Naphthalene. *Environ. Sci. Technol.* **2009**, *43*, 1349-1353.
5. Smith, D. F.; McIver, C. D.; Kleindienst, T. E. Primary Product Distribution from the Reaction of Hydroxyl Radicals with Toluene at ppb NO_x Mixing Ratios. *J. Atmos. Chem.* **1998**, *30*, 209-228.
6. Smith, D. F.; Kleindienst, T. E.; McIver, C. D. Primary Product Distributions from the Reaction of OH with *m*-, *p*-Xylene, 1,2,4- and 1,3,5-Trimethylbenzene. *J. Atmos. Chem.* **1999**, *34*, 339-364.
7. Bethel, H. L.; Atkinson, R.; Arey, J. Products of the Gas-Phase Reactions of OH Radicals with *p*-Xylene and 1,2,3- and 1,2,4-Trimethylbenzene: Effect of NO_2 Concentration. *J. Phys. Chem. A* **2000**, *104*, 8922-8929.

8. Gómez Alvarez, E.; Viidanoja, J.; Muñoz, A.; Wirtz, K.; Hjorth, J. Experimental Confirmation of the Dicarbonyl Route in the Photo-Oxidation of Toluene and Benzene. *Environ. Sci. Technol.* **2007**, *41*, 8362-8369.

9. Arey, J.; Obermeyer, G.; Aschmann, S. M.; Chattopadhyay, S.; Cusick, R. D.; Atkinson, R. Dicarbonyl Products of the OH Radical-Initiated Reaction of a Series of Aromatic Hydrocarbons. *Environ. Sci. Technol*. **2009**, *43*, 683-689.

10. Aschmann, S. M.; Arey, J.; Atkinson, R. Rate Constants for the Reactions of OH Radicals with 1,2,4,5-Tetramethylbenzene, Pentamethylbenzene, 2,4,5-Trimethylbenzaldehyde, 2,4,5-Trimethylphenol, and 3-Methyl-3-hexene-2,5-dione and Products of OH + 1,2,4,5-Tetramethylbenzene. *J. Phys. Chem. A* **2013**, *117*, 2556-2568.

11. Atkinson, R.; Aschmann, S. M. Products of the Gas-Phase Reactions of Aromatic Hydrocarbons: Effect of NO_2 Concentration. *Int. J. Chem. Kinet.* **1994**, *26*, 929-944.

12. Volkamer, R.; Spietz, P.; Burrows, J.; Platt, U. High-Resolution Absorption Cross-Section of Glyoxal in the UV-Vis and IR Spectral Ranges. *J. Photochem. Photobiol. A: Chem.* **2005**, *172*, 35-46.